

**UNCLASSIFIED**

**AD NUMBER**

**AD011549**

**CLASSIFICATION CHANGES**

TO: **unclassified**

FROM: **restricted**

**LIMITATION CHANGES**

TO:

**Approved for public release, distribution  
unlimited**

FROM:

**Distribution authorized to U.S. Gov't.  
agencies and their contractors; Foreign  
Government Information; 16 AUG 1952. Other  
requests shall be referred to British  
Embassy, 3100 Massachusetts Avenue, NW,  
Washington, DC 20008.**

**AUTHORITY**

**DSTL, DSIR 23/20965, 30 May 2008; DSTL,  
DSIR 23/20965, 30 May 2008**

**THIS PAGE IS UNCLASSIFIED**

Reproduced by

Armed Services Technical Information Agency  
DOCUMENT SERVICE CENTER

KNOTT BUILDING, DAYTON, 2, OHIO

AD -

11549

RESTRICTED

AD No. 11549

ASTIA FILE COPY

13, 125

卷之三

ENRICK, HOLLOWAY

卷之二

## STRUCTURE SUB-COMPONENT

Struct-1-64

**AGRICULTURAL RESEARCH COUNCIL.**

## An Experimental Study of a Transversely Stiffened Tapered Box Girder under Torsion and Bending.

- By -  
Kruso Maloro Falooner, B.E., A.R.D., D.I.C.

Commissioned by Prof. Dr. J. Sutton (Finspång)

16th August, 1911.

### Summary

This paper describes an experimental investigation, carried out in the Civil Engineering Laboratories of the Imperial College of Science and Technology, of the strain distribution in a transversely stiffened tapered box of trapezoidal cross section under torsion and bending. The overall length of the box was 16 ft. 3 in. and the wall thicknesses were sufficient to prevent the plating from buckling under test loadings.

The distributions of direct and shear strains around representative cross sections are shown graphically. For comparison with existing theory, curves have been superimposed showing the strains according to the engineers' theory of bending, the Freud-Haftke theory of torsion, and the general theory of Argyris and Lunge. Two analyses have been made from the latter theory - one as an 'equivalent four beam tube', and the other as a tube with 'direct stress carrying covers'.

	Page
1. Introduction	2
1.1 The present investigation	2
1.2 Existing theories	3
2. Scope of the Investigation	3
3. Choice of Test Box	3
4. Description of the Test Box	4
5. Loading Apparatus	5
6. Measurement of Strain	6
7. Experimental Strains	7
8. Computed Strains	8

**Best  
Available  
Copy**

	Page
9. Discussion of Results	12
9.1 General	12
9.2 Elementary theories	13
9.3 Theory of Argyris and Danno	14
10. Conclusions	15
Photographs	
Figures	
Tables	
APPENDIX I	
APPENDIX II	
1. Introduction	

A number of theoretical papers have drawn attention to the limitations of the conventional engineers' theories of bending and torsion commonly used for finding the stress distribution in stressed skin tubular structures. These theories are strictly applicable only for long members of uniform cross section and do not apply in the regions of loads and restraints. Their simplicity, however, has encouraged their extension to structures where the premises are known to be invalid.

The more general theories, which have been presented to consider the effects of taper and the proximity of loads and restraints, must be judged both by their accuracy and their simplicity of application to particular structures. The present investigation has been designed to provide information for use in examining the basic premises of the new theories, and to assist in determining the range of usefulness of the conventional theories.

Prototype wing tests, as normally carried out, do not provide suitable data for this purpose as the stress distribution in actual wing structures is complicated both by buckling and by structural discontinuities, in addition to the characteristics which it is required to study. Furthermore the main purpose of full-scale wing tests is to establish the ultimate strength of the structures, and strain measurements have not been measured in sufficient detail for the present purpose.

#### 1.1 The present investigation

The present investigation was proposed by the Structure Sub-committee of the Aeronautical Research Council, who desired a detailed record of the strain distribution in a moderately tapered unswept box, which could be used, in particular, for an examination of the basic assumptions of the general theory of tubes published by Argyris and Danno<sup>1</sup>. The maximum angle of taper of the box was limited to about ten degrees, owing to a restriction imposed by a premise of the general theory.

<sup>1</sup>The General Theory of Cylindrical and Conical Tubes under Torsion and Bending Loads, by J. Hadi Argyris and G. C. Danno, Journal of the Royal Aeronautical Society, 1947.

A special test specimen without structural discontinuities was designed for the test. In order that it should behave linearly with load, the skin thicknesses, though large in comparison with normal aircraft practice, were chosen so that buckling would not occur under test loadings. The structure has been tested under pure torsion and under combinations of bending and torsion. The results are presented graphically at the end of the report.

The work was carried out in the Civil Engineering Laboratories of the Imperial College of Science and Technology, London.

#### 1.2 Existing theories

Although the problem of finding the stress distribution in tubular structures can be formulated in terms of the expressions of the classical theory of elasticity, a thorough theoretical analysis has not yet been made because of the very great difficulties encountered in mathematical development. It seems probable that numerical solutions could be obtained by successive applications of relaxation methods but unfortunately these would lack generality.

In existing theories the problem has been rendered tractable by assumptions which simplify the elastic properties of the construction material and prescribe the modes in which deformation may be considered.

It is a fundamental assumption of the conventional beam theory that the distributions of direct strains over cross sections are linear. With this assumption the basic problem is to determine the deflection of a line joining the centroidal axes of cross sections; one does not then have to consider the elastic deformation of the three-dimensional structure. In the Bredt-Batho theory of torsion, it is presumed that a purely torsional component of load at any cross section is dissipated as a constant shear traction which acts tangentially around the perimeter. With both these assumptions it has been found possible to calculate stress distributions from Hooke's Law and the equilibrium equations of statics.

It is reasonable to presume from the principle of Saint Venant that at regions remote from loads, restraints, and discontinuities, the stress distributions of the conventional theory approach the actual stress distributions. Unfortunately in aircraft structures the aspect ratio of components is often low and it is seldom possible to apply Saint Venant's Principle with any real justification. As the highest stresses usually occur in the region of loaded and restrained sections, the conventional or elementary theories are often not sufficiently accurate.

In recent years theories have appeared which allow a more general mode of deformation under load than is permitted by the conventional theories. Attempts have been made to compute skin stresses which satisfy the stress strain relationships of the theory of elasticity, but in general this requirement has been too stringent. However a great simplification can be introduced by assuming zero transverse direct stress and strain in the skin. As a result only one equation for the equilibrium of an element of the material need be considered. From such a premise, and by assuming an idealised geometrical form, Argyris and Duffe have evolved their general theory of tubes under torsion and bending loads.

#### 2. Scope of the investigation

The objects of the investigation have been to find the strain distribution in a moderately tapered, transversely stiffened, thin-walled duralumin box under torsion and bending, and to give a comparison with the strains calculated by the conventional engineers' theories and the general theory of Argyris and Duffe.

Plate 1 and Fig.1 show the box which was built to fulfil, as closely as possible, the assumptions of the Argyris and Durne theory. The box was symmetrical about its central transverse plane as in an aeroplane wing, to assure complete axial constraint at the central cross section under symmetrical loadings, and to afford the possibility of check measurements in the second half of the structure.

The box was tested in bending, in pure torsion, and in bending plus torsion. The loads were applied successively at the tips and at the third points between the tip and root sections, and were reacted at the central cross section.

Distributions of direct and shear strains were measured around representative cross sections, with the use of electric resistance strain gauges fitted as in Fig.4. The measurements have been plotted in a standard form using the perimeter of cross section as a base, and theoretical strains have been superimposed in order to give a pictorial comparison of results. Two analyses have been made from the Argyris and Durne theory - one as an 'equivalent four box tube' and the other as a tube with 'direct stress carrying covers'.

The choice of a test box is discussed in Part 3, and a description of it is given in Part 4. The test frame and loading rig are described in Part 5, the experimental technique in Part 6, the strain measurements in Part 7, and the analytical treatment in Part 8. A brief non-mathematical review of the Argyris and Durne theory is given in Appendix II.

### 3. Choice of a Test Box

It is common in the design of aircraft structures to assume that thin plating can only resist shear stresses. Portions of the plating which would otherwise have carried direct stresses may then be allotted to booms and stringers on the basis of an effective width theory. In cases where this procedure is accepted the theory of Argyris and Durne finds its simplest application. The payout factor is tolerably easy for tubes having from four to six booms, though it can become prohibitive when the booms are numerous.

Though such an application of the theory may be of greater practical importance than the more general treatment, and the departures from elementary theory due to shear lag and other effects can be much greater when longitudinal stiffening is present, it was considered undesirable to use such a box for the present project. For example, the present arbitrary allocation of plate areas to booms and stringers could lead to large errors if the plates were thick. However if the walls were sufficiently thin for their influence on the direct stress distribution to be apparently insignificant, they would surely buckle; this would cause the box to behave non-linearly and would complicate the experimental analysis unduly.

While from practical considerations of computation according to the Argyris and Durne theory, it would have been convenient to test a four-boomed tube with very thin walls, for the foregoing reason this was not done. Furthermore, the practice of the shear-stress-direct-stress allocation noted above, would introduce an assumption which is not fundamental to the general theory, but has merely been introduced for convenience in computing particular cases. Mathematically the assumption is equivalent to replacing a continuous function by a number of discrete steps and, unless the individual steps were small and sufficiently numerous, this could introduce appreciable error.

The box used had transversely supported walls sufficiently thick not to buckle, and small corner angles; this was considered to be the best of the alternatives which could be conveniently constructed. The chosen taper was the greatest to which it was considered the theory could be reasonably applied for the purpose of the present investigation. The overall size was determined from considerations of taper, constructional limits, workmanship, size of available strain gauges, and the minimum convenient spacing of transverse diaphragms which would allow gauges to be fitted on the inside of the box after three sides had been assembled with the fourth left off for access. The thickness of the plating was chosen so that its critical buckling stresses would be appreciably higher than the working stresses, and any initial deflections of the plating would be very small fractions of the plate thickness.

#### 4. Description of Test Box

The test structure was a box girder of trapezoidal cross section having a length of 16 ft. 3 in. and made of DMD.610 B duralumin. It was symmetrical about its central cross section and tapered linearly towards each tip so that the longitudinal generators of the surface met in common points beyond the ends of the box. The box is shown in Plate 1, and various details of the internal construction are shown in Plates 2 - 4.

At the centre of the structure a heavy, mild steel, box component having reinforced holes, was built inside the skin to permit access to strain gauges on the inner surface at the root. This steel structure had three parallel diaphragms, as shown in Plate 2. Because of its high rigidity, the cross sections which are alongside the outer diaphragms and contain the outer rows of rivets were regarded as axially constrained 'root cross sections' of the outboard portions of the box. Access to the inside was possible through holes in the covering between the inner and an outer diaphragm, and in the outer diaphragm.

At the tips and at the third-points between tip and root, mild steel diaphragms were fitted for dispersing the applied loads into the structure. These loading diaphragms may be seen in Plates 2 and 4, and eye-bolts which screwed into them through holes in the cover, are shown in Plates 1 and 4. The transverse shape of the box was maintained by duralumin diaphragms, spaced at uniform intervals along the length of the structure: these were parallel to the 'root cross sections' and also the central cross section.

The central line of the rear spar was a straight line from tip to tip of the box, and the tip cross sections were half way between taper points and root cross sections. The principal dimensions of the structure are given below and in Fig. 1.

Overall length	16 ft. 3 in.
Distance between root cross sections	15 in.
Distance from root to tip cross sections	90 in.
Spacing between loading diaphragms	30 in.
Spacing between stabilizing diaphragms	6 in.
Distance between spars at root	30 in.
Depth of front spar at root	12 in.
Depth of rear spar at root	8 in.
Distance between spars at tip	15 in.
Thickness of covers	0.190 in.
Thickness of spars	0.157 in.
Thickness of webs of stabilizing diaphragms	0.030 in.
Thickness of webs of loading diaphragms	3/8 in.
Thickness of plating of central stiffening structure	1/2 in.

The spar web plates were flanged outwards at their edges and were joined to the covers by steel rivets (Plate 4). The length of leg of the 'corner angles', so formed, was kept as small as practicable. By suitably selecting rivet sizes and pitches the leg length was allowed to taper towards the tip in approximately the same manner as the rest of the box. The riveting at the corner angles can be seen in Plate 4.

In order that the diaphragms should offer the minimum of restraint to warping under load, the attachment angles of the stabilizing diaphragms and the flanges of the loading diaphragms were slotted at intervals around their perimeters, as shown in Fig.2. To increase the rotational restraint of the diaphragms against buckling of the covers, the legs of the diaphragm attachment angles were propped from the web stiffeners as shown in Plate 3.

The central stiffening structure and the loading diaphragms were welded mild steel plates and the surfaces in contact with the skin were machined to a tolerance of 0.012 in. Light alloy castings would have been too costly and similar components of riveted construction would have been too cumbersome. It is probable that temperature stresses were introduced by the differing thermal coefficients of expansion of steel and duralumin but this was accepted as of little consequence, since the structure behaved linearly with load and cycles of strain readings were taken under practically constant temperatures.

The test loads were transmitted to the structure by high tensile steel eye-bolts, which were screwed into blocks of mild steel welded in line with the webs of the loading diaphragms, as shown in Plate 2. The applied loads were transferred from the blocks into the diaphragm webs and then dispersed around the perimeters. Only small distortion within the plane of cross section should have occurred at the loading diaphragms, as the shear rigidity of the steel webs was equivalent to that of duralumin one inch thick.

To decrease the influence of the access holes upon the stress distribution nearby, stiffening straps were welded around the periphery of the holes on the inside of the central steel structure, and then joined to the central diaphragm so that the straps in effect bounded each adjacent pair of holes. In addition the central steel structure was made of half-inch plate and so was very stiff in comparison with the rest of the box. The half-inch steel plate and duralumin covering had a combined rigidity equivalent to duralumin 1.1 in. thick. These precautions ensured that the access holes had a negligible influence on the stress distributions at the root cross sections.

To limit the possibility of rivet slip at the root cross section, the covers and spars were made of continuous sheets from tip to tip of the box, and additional external cover plates were fitted over the region of the central stiffening structure. The front spar of the box was fitted last. Solid rivets were used for all connections except at the junctions of the diaphragms and the front spar where hollow Chubbert rivets were used. The design and construction of the test box required the greatest care and thanks are due to the Fairey Aviation Company, who made the box, for maintaining a high standard of craftsmanship throughout.

### 5. Loading Apparatus

As a preliminary to the investigation, it was necessary to build a space frame for loading the box. Though the frame and loading apparatus have been made of a size and capacity convenient for the present test, they were designed for general use in structural testing and now remain as a part of the permanent laboratory equipment. The test frame can be used for applying up to four tensile loads of 10 tons each, in vertical or transversely horizontal directions, anywhere within a space of 22 x 9 x 9 ft. In addition, one single tensile 50 ton load, or two orthogonal or two tensionally opposed tensile loads of up to 50 tons each, can be reacted in the central transverse plane of the structure.

As may be seen in Plate 3, the space frame consists of four parallel and vertical portal frames, which are set at right angles to their common longitudinal axis and then joined together. The truss is carried externally on outriggers so that it will be clear of the loading apparatus. The laboratory floor is of timber on steel joists above a basement, and all live loadings had therefore to be equilibrated with the frame.

Loads are applied by hydraulically operating jacks supported on beams spanning from an outer to an inner frame. The jacks can be moved along the beams, and the beams can be moved around the perimeter of the portal frames, as required. At ground level there is a control panel with an array of needle valves for operating the jacks, either individually or collectively. Measurements of load are made with statimeters and a proving ring; the latter is also used to recalibrate the statimeters at intervals during tests. It is estimated that the loads in the present investigation were measured within an error of 2%, or 150 lb which ever was the greater.

The test box was supported at its centre by four steel straps lying in the central transverse plane of the structure. So that the girder could be free to 'see saw' about its centre, the straps were pin-jointed with universal links close to the girder. Under a very light push the tip could be moved up and down by 2 to 3 in.

The linkage for applying the test loadings is shown diagrammatically in Fig. 1 and may be seen in detail in the various photographs. It was made mainly of high tensile steel and has the same load capacity as the test frame, for subsequent general use. The linkage is constructed so that its dead weight is not applied to the test box, and so that the forces at the measuring instruments are either equal to the applied loads, or a fixed ratio of them, and did not require zero corrections.

The box was loaded symmetrically, at a cross section on each side of the transverse centre plane, by forces statically equivalent to a vertical shear and a twisting moment in planes of application parallel to the root cross sections. The combined components of load were reacted at the centre by the four straps supporting the girder. As the straps could only resist tension four of them were necessary.

The applied loading is shown in the upper diagram of Fig.2 and the linkage chosen to obtain it in the lower diagram. If a symmetrical arrangement of jacks had been used, noting as in the upper diagram, then the shear component of load,  $V_F$ , could have had to be found from the differences in readings of the measuring instruments for the upward and downward loads. The percentage error in  $V_F$  might then have been much higher than the error in  $F$  or  $F + V_F$ , particularly when  $\Delta F$  was small.

Since the component of load  $V_F$  produced the bending strains at the root, it was necessary to know its value within the same percentage error as the load  $F$ . This was possible with the linkage arrangement adopted as  $\Delta F$  was measured directly. Further the orthogonal arrangement of forces ensured that the loads applied by the two horizontal jacks were equal, and, except for effects of elastic deformation of the box and test frame, were unaffected by slight vertical movements of the test structure. This was a great advantage, as the jacks operated at four separate pressures in order that the ratio of loads could be changed at the control panel. When adjusting the loads only three of the jacks needed to be operated. After a little practice each instrument could be adjusted for full load in about 15 sec.

#### 6. Measurement of strains

Electric resistance strain gauges were attached around the root cross sections on both sides of the central stiffening structure and at five additional cross sections in each half of the box. Two of these were located on either side of the innermost loading dipper, and the remaining three centrally in the three spaces between the loading dipper arms and the root cross section.

The location and distribution of gauges is shown in Fig.4. Standard single element wires (Inalyte type No. 100 ohm per in. gauge length) were used, as rosette strain gauges were not available. They were attached in patterns of longitudinal and inclined gauges, to measure linear strain along, and at 45° across to the generators respectively. Gauges were placed, with the same orientation, on both the inner and outer surfaces of the plating, and the distributions were symmetrically disposed about the centres of the sides of cross section. Before attaching the gauges paper templates with rectangular holes cut in the desired patterns were glued on the inner and outer surfaces of the plating. The templates were located from  $1/16$  in. holes drilled through the plating at the ends of cross section sides, and the gauges were glued within the rectangles as may be seen in Plates 3 and 4.

Measurements of strain were made with a Baldwin-Worthmark, 5000 channel scanner recorder, recording synchronically on circular charts. One thousand strain gauges are used, arranged in groups of forty. Each group is wired to a plug of an improvised forty point mercury switch, the bases of which are connected permanently to forty channels of the recorder. By interchanging the plugs which fitted in the base, particular groups of gauges were quickly and easily selected for recording. The loading cycles had to be repeated for each plug until all desired measurements were recorded. The arrangement is shown in Photo 2.

It was intended to reduce the labour of 'zero balancing' the gauge resistances prior to measurement, by using gauges with only a small tolerance of  $\pm 0.2$  ohms on their nominal resistance of 100 ohms, and also by using only specially selected gauges of 100.0 ohms as dummy's. Unfortunately, after all gauges were fixed and the wiring was completed the resistance tolerance was found to be about  $\pm 0.6$  ohms which was too large for the measuring instrument.

An attempt was then made, by soldering short lengths of resistance wire in series with each gauge, to adjust all gauges plus their pairs of wires to within  $\pm 0.05$  ohms of a nominal resistance of 101 ohms. Had this been successful the labour of obtaining readings would have been approximately halved, since zero balancing would not have been necessary, as all readings would have been within the scale of the recorder charts. It was not fully achieved, but a great improvement was made and most gauges were finally within  $\pm 0.2$  ohms and at least half were within 0.1 ohm.

A calibration beam was used to check the reading of the recorder and the behaviour of sample gauges. No allowance was made for lateral sensitivity of the gauges, believed to be about 2% of the lateral strain. The strains were measured within an estimated error of  $\pm 5 \times 10^{-3}$ .

As a visual aid in reading the strains which had been recorded graphically on the circular charts of the Baldwin instrument, a turntable device was made having a scale of strain mounted on a quadrant arm. This may be seen slightly right of centre in PLATE 9. The quadrant pivoted about the same relative point as the pen arm of the recorder. By rotating it until the zero of its scale coincided with the 'baseline' reading made at zero load, the scale could be read directly, without the inconvenience of continually subtracting slight errors of the zero setting.

The test results are first plotted on graphs as shown in Figs. 5-7, which for convenience had been printed for each cross section with the grid lines and gauge orientations shown on the paper. Curves were drawn through the test results for similarly orientated gauges, mean values being taken for inner and outer curves. The results were then replotted on graphs showing the full cross section. Axial direct strains were plotted directly; shear strains were plotted from the vertical intercepts between the curves for inclined gauges.

#### 7. Experimental Strains

The test structure was loaded with concentrated forces applied at the tips and at the third points between tip and root sections. The forces were symmetrically disposed about the central cross section of the box and lay in planes parallel to the root cross section. They were transmitted to the box through the eye-bolts indicated in Fig. 1 and shown in Photo 1. Conditions of loading ranged from vertical shears which mainly produced bending, through combined shear and torsion, to pure torsion.

Strains were measured at sections 1 to 7 of Fig. 1. The results are shown graphically in Figs. 8 to 14. For convenience these have been shown in a standard form, using the perimeter of cross sections as a base. The loadings, measurement sections, and corresponding figure numbers of results are given in Table 1.

Table 1

Loading at cross section 2/3 of distance from tip to root

Load	here applied	measured at section	shown in figure
20,000 lb	front eye-bolt	A, B, C, D	8, 10, 12, 14
15,000 lb	" "	D	15
20,000 lb	rear eye-bolt	A, B, C,	9, 11, 13, 15
15,000 lb	" "	D	17
8,125 lb	one chord out from rear spar	A, B, C, D	37, 39, 41, 42
400,000 lb in.	(pure torque)	A, C, D	36, 40, 42

Loading at cross section 1/3 of distance from tip to root

Load	here applied	measured at section	shown in figure
40,000 lb	front eye-bolt	A, B, C, D	18, 20, 22, 24, 26, 28
40,000 lb	rear eye-bolt	A, B, C, D	19, 21, 23, 25, 27, 29
7,000 lb	One chord out from rear spar	A, B, C	45, 47, 49
300,000 lb in.	(pure torque)	A, B, C	44, 46, 48

Loading at tip cross section

load	here applied	measured at section	shown in figure
6666 lb	front eye-bolt	A, B, {C, E, F}	30, 32, {34}
6666 lb	rear eye-bolt	A, B, {C, E, F}	31, 33, {35}

The experimental results for the box loaded principally in shear, that is by a single vertical force applied directly to an eye-bolt on each side of the central cross section, were obtained before the linkage for torsional loadings had been constructed. It can be seen from these that measurements made at sections A and B under the same loading conditions agreed very closely. The agreement as shown by comparison of Figs. 5 and 10, of 9 and 11, of 16 and 20, and of 19 and 21, was such that this was not tested in later tests in taking readings on both sides of the central cross section of the box.

As an aid in comparing results, the bending loads of 6666, 10,000 and 20,000 lb which were applied at the respective loading sections, had been chosen to produce the same bending moment, of 600,000 lb in. at the root cross section. The maximum stress corresponding to this moment was 34.00 p.s.i. (according to elementary theory) and was appreciably less than the critical compressive stress of the cover plating due to the bending of the box (at least 9000 p.s.i. calculated on the assumption that the diaphragms gave only simple support to the covers).

It may be of interest to note that, though the construction was very good and maximal initial deflections of the plating only about 3% of its thickness, a number of the strain gauge results indicated that slight buckling occurred in some places at well below the critical stress. The 'buckling' was noticed most of all at section B when the 6666 lb loads were applied at the tip. Dual deflection gauges showed it to be  $40 \times 10^{-4}$  in. between diaphragms, or 2% of plate thickness, and to have increased approximately linearly with load.

Apart from the slight discrepancy in surface strains, the box behaved linearly with load. To help confirm this the results shown in Fig. 51 were predicted by superimposing components found by taking the required fractions of Figs. 10 and 11 in order that the combined loadings could be statically equivalent to the loading of Fig. 51. The prediction, shown in Fig. 50, is reasonably close.

On completion of the tests it was found that of the 1056 electro-resistance strain gauges fitted to the base only 21 were defective because of open circuits or large apparent zero drifting. Most of the defective gauges were on the inside of the box and had been damaged initially during assembly of the fourth side. It is perhaps remarkable that of the 1035 remaining serviceable gauges, measurements from only one have been ignored in plotting the results. This gauge was located inside the box on a cover at Section B, and consistently gave high readings under load, even though zero readings were repeatable. The readings from the corresponding gauge on the outer surface agreed with the trend of results from adjacent gauges on both sides of the plating.

#### 5. Computed Strains

Strains have been computed both by conventional elementary theories and by the general theory of Argyris and Durrne. They have been plotted on the same graphs as the experiment 1 results, to give a pictorial comparison between theory and experiment. The method of plotting will be understood by reference to the figures.

No attempt has been made to obtain 'experimental' stresses from measured strains, as it is considered more fundamental and simpler to compare measurements and computations directly. It may, however, be of interest to note that a strain of  $4 \times 10^{-4}$  in dual-gauge is equivalent to a unidirectional stress of 4000 p.s.i. (1.72 tons per sq.in.) or a shear stress of 1500 p.s.i. (0.696 tons per square).

A brief record of the computations is given in Appendix II. Two analyses have been made using the general theory of Argyris and Durrne - one treating the box as an 'equivalent four beam tube', and the other as a 'tube with direct stress carrying covers'.

Strains derived from the former analysis are shown on all diagrams of results. Where the computed stresses are too small to plot, or the curves may be confusing, the results have been tabulated alongside each graph. Strains from the latter analysis have been shown only against the results for torsion, and such other results where they appear to be significant. They are given fully in Table 4 for all loadings close to the root cross section.

## 9. Discussion of Results

### 9.1 General

As cross sections of the box have a horizontal axis of symmetry, the distributions of theoretical strain in the upper and lower halves are symmetrical in magnitude. Because of the sign convention adopted in plotting, the shear strains are of like sign and the direct strains of opposite sign. Inspection of the graphs shows close agreement between the experimental results for top and bottom covers and for the upper and lower halves of the spar webs. This confirms that the straining was linear with load.

An exception to this symmetrical behaviour is shown by the direct strain in the front spar web at Section C for loadings of Figs. 14 and 40. The deviation, which was checked by repeating the measurements, is not considered to be due to misbehaviour of the electric strain gauges on the web at that section, as the results shown in Figs. 24 and 25 are satisfactory. It may be caused by rivet slip or deformation in the neighbourhood of the loaded section, since the front spar was fitted last and hollow Chobert rivets had to be used to attach it to the internal diaphragms. Such behaviour does not occur at Section A, where it was possible to use solid rivets on all four sides of the root cross section, because of the proximity of the access holes.

In general the experimental results lie along continuous curves and relatively small individual scatter is apparent, and it may be inferred that the results are a faithful record of the straining of the box.

A general trend of the experimental results for 'shear' loadings shown in Figs. 8-11 is that the magnitudes of shear strain in the covers are given by lines of reverse curvature, whereas lines of single curvature are predicted by the elementary theories. The minimum slope of the experimental lines occurs at about the centre of the covers, where it is about half that of the elementary theories. The slope tends to remain constant over a central band about half the width of the covers, and then to increase towards the corners of the sections. This is particularly evident for loadings close to the root. As may also be seen from the graphs, the effect of altering the torsional exponent of the 'shear' loading is to displace the curve of shear strain frx. the base line by constant increments.

It may appear from Figs. 8 and 10, that the lines of experimental shear strain shown in the front spars are more sharply curved than is consistent with the large rate of change of direct strains with depth of the spar web.

Large appreciable deviation from linearity of direct strain over cross sections of the covers is evident for loading close to the root. At sections P and A of Figs. 8-11 a large decrease in direct strain was recorded near the centre of the covers, whilst at section C and D of Figs. 11 to 17 there was a large increase. For the other two sections where loadings deviated from linearity were very greatly reduced.

The experimental shear strains for pure torsion tend to remain constant in each wall of the box. This is particularly evident in the results for sections B and E of Figs. 8 and 12, where the distribution of strain is very simple. Greater deviations from uniformity of shear strain have been found for torsional loadings applied nearer the root.

Thy/

The 'torsion bending' direct strains, which have developed for the pure torque loadings, appear to be self equilibrating. They are of anticipated sign and are larger for the loading nearer the root.

The results for shear plus torque show characteristics of each loading.

#### 9.2 Elementary theories

Figs. 22, 47 and 46 have been obtained for Section B when loadings of 'shear', torque plus shear, and pure torque respectively were applied at  $\alpha = 120^\circ$ . Section B was reasonably remote from loads and restraints, and examination of the results shows that the elementary theory has very good accuracy for each of the three loadings. Because of the statical equivalence of theoretical and true stresses, it can be seen that the shears, moments, and torques corresponding to the experimentally measured strains must have been in equilibrium with the applied loads. Hence the experimental technique was satisfactory, and the values of direct and shear moduli of elasticity found initially from tests of specimens of the material, and which were used in computation, remained representative of the fabricated structure.

A detailed comparison of theory and experiment may be made by studying the figures.

It is interesting to note where the maximum experimental shear strains differ appreciably from the maximum strains of the elementary theories. In Table 2 the differences, expressed as a percentage of the theoretical values, have been listed where those exceed 5 per cent. As the direct strains due to torque have no elementary theoretical values they have been listed, instead, as percentages of the single theory shear strains. In Fig. 36 the experimental shear strain is intermediate between the elementary and general theoretical values, whilst in Figs. 40 and 41 the general and experimental values are in close agreement. This is of importance as the greatest deviations, 3% for pure torsion and 2% for torsion plus bending, have been found immediately inboard of the loading section at  $\alpha = 15^\circ$ .

Table 2

Figure No.	Percentage deviation of maximum experimental strains from maximum strains of the elementary theories		
	Shear	Direct	Direct (due to pure torque)
8	+ 7	+ 20	
9		+ 9	
10	+13	+ 20	
11		+ 12	
12		+ 6	
14		+ 50	
15	+ 8	+ 6	
20	+ 9	+ 9	
22	+ 5		
36	+11		+35
37		+ 75	
39	+ 8		
40	+ 24		+25
41	+31	+350	+20
44	+10		+40
45	+ 5		
46			+19
47	+ 7		
48		+ 75	+13
49			

After the main tests were completed two inclined gauges, which may be seen at the upper left hand corner of Photo 9, were fixed on the outer surface of the rear spar wet immediately inboard of the loading section at  $r = 120^\circ$ , as large deviations can be expected immediately inboard of inner loading sections. The readings from these two gauges indicated deviations of about +30% in shear strain for the torsional loading.

#### 9.3 Theory of AIAA and Dorn

The computation for an 'equivalent four book tube' was intended to give a first approximation to components of the self-equilibrating stresses due to torsional components of load. In this treatment the distribution of direct stress in each wall is presumed to be linear and shear lag and related effects are ignored. The computation for a tube with 'direct stress carrying covers', however, has been intended to give the self-equilibrating stresses for both torsional and shear components of load.

From the results it can be seen that both treatments have given a fair estimate of the stresses due to torsional loadings, but the second treatment has not interpreted the 'lagging' of measured strains under shear loadings, as may be seen from Table 8. Analytical results from the second treatment have not been plotted on the graphs for shear loadings, except for the webs of Figs. 3 and 9. For the loadings at  $\theta = 150^\circ$  the theoretical results of the second treatment have been listed in Table 6.

The results for pure torsion at  $\theta = 150^\circ$  are of interest as they show strain distributions close to the root and on each side of the loading section. At the root the torsion bending strains are in close agreement with the theory, though the shear strains are smaller than predicted, and are intermediate between those of the general and elementary theories. On each side of the loading section the shear strains of experiment and the general theory are in very good agreement, as may be seen in Figs. 40 and 42. This is of great importance as the recorded shear strain in the rear spar web immediately inboard of the loading section (see Fig. 40) is about 3% greater than is predicted by the Bredt-Betha theory.

The results for loadings combining torsion and shear exhibit characteristics of both the shear and torsion solutions.

The lateral straining of the plating was very small, and is consistent with the assumption that it is sufficiently small to be ignored. The lateral strain at the measurement sections could be obtained quite simply from the graphs of linear strains, such as shown in Figs. 5 to 7, by subtracting the axial direct strain from the sum of the two inclined linear strains which had been measured in orthogonal directions. From Figs. 5 to 7 it can be seen that the lateral strain is close to zero, yet of opposite sign to the axial direct strain, as would have been expected from the Poisson effect. Although the lateral straining remains less than the Poisson value, because of the transverse restraint of the diaphragms, it is considered that the transverse stress as well as strain is sufficiently small to be ignored.

#### 4. Conclusion

The test structure was built to fulfil, as closely as possible, the assumptions of the general theory of springs and frames. It had, therefore, a moderate end critical taper and an stiffened with closely spaced transverse diaphragms. The thickness of plating prevented buckling, and the structure behaved linearly with loads.

An important assumption of the general theory is that both the transverse direct stress and strain are zero. This, though an apparent anomaly is considered justifiable as the results show that both quantities are sufficiently small to have been ignored. As anticipated, the error of the elementary theories is larger for loadings nearer the roots. Under the shear loads the maximum direct strain at the root exceeded those predicted from the conventional beam theory by up to 20%, and under torque the maximum shear strain immediately inboard of the innermost loading section exceeded that of the Bredt-Betha theory by 3.5%.

The computation for an 'equivalent four beam tube' was comparatively simple and could have been completed in a week, whilst the computation and tabulation of results for the 'tube with direct stresses carrying covers' was laborious and required approximately 100 man hours. Both computations give an equally good estimate of the strains due to torsional loadings. The four beam assumption could not of course interpret the strain lag when shear loads were applied and this was the chief reason

for making the required more complex analysis. Unfortunately the latter has still not done so. It is probable that some estimate of the lag in strain could be obtained by analysing the box as an 'equivalent eight boom tube' having four equally spaced 'booms' across each cover.

The analysis for four boom tubes, because of its relative simplicity, should prove useful in estimating the stresses due to torsion of tubes with quadrilateral cross sections. It seems reasonable to state that the accuracy will be higher when corner booms are present though some experimental confirmation of this is desirable.

#### Acknowledgements

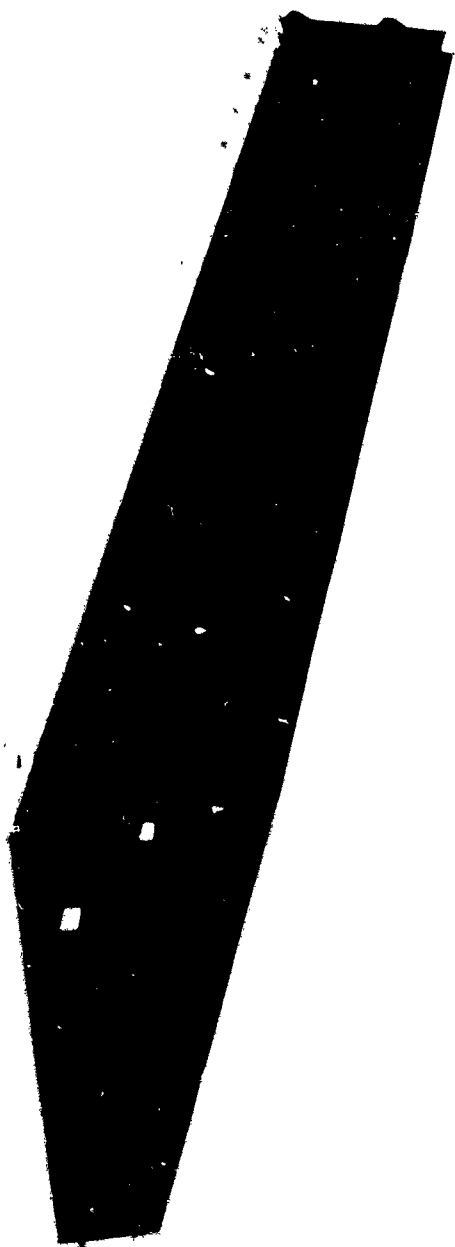
The author is indebted to Prof. A. J. S. Lippard and Dr. S. N. Sparkes of the Imperial College of Science and Technology for the opportunity and facilities for doing the work and for help and encouragement during its progress.

He also wishes to record his gratitude to the Ministry of Supply for providing the test box, to the Department of Scientific and Industrial Research for a grant covering the test frame and assistance, to Mr. T. P. E. George and others of the Fairey Aviation Company for help during manufacture of the test box and components of the loading linkage, to the Director of the Royal Aircraft Establishment for the loan of electrical strain measuring equipment and to Mr. C. P. G. Bateman and Mr. J. Heale for assistance in planning and testing. Mrs. B. H. Falconer did much on the curve-plotting, and Miss E. Horton made many of the detailed computations.

Finally thanks are due to Mr. J. C. Chapman for numerous invaluable discussions during the course of the project.

15-128  
Plate I

The Tapered Test Box

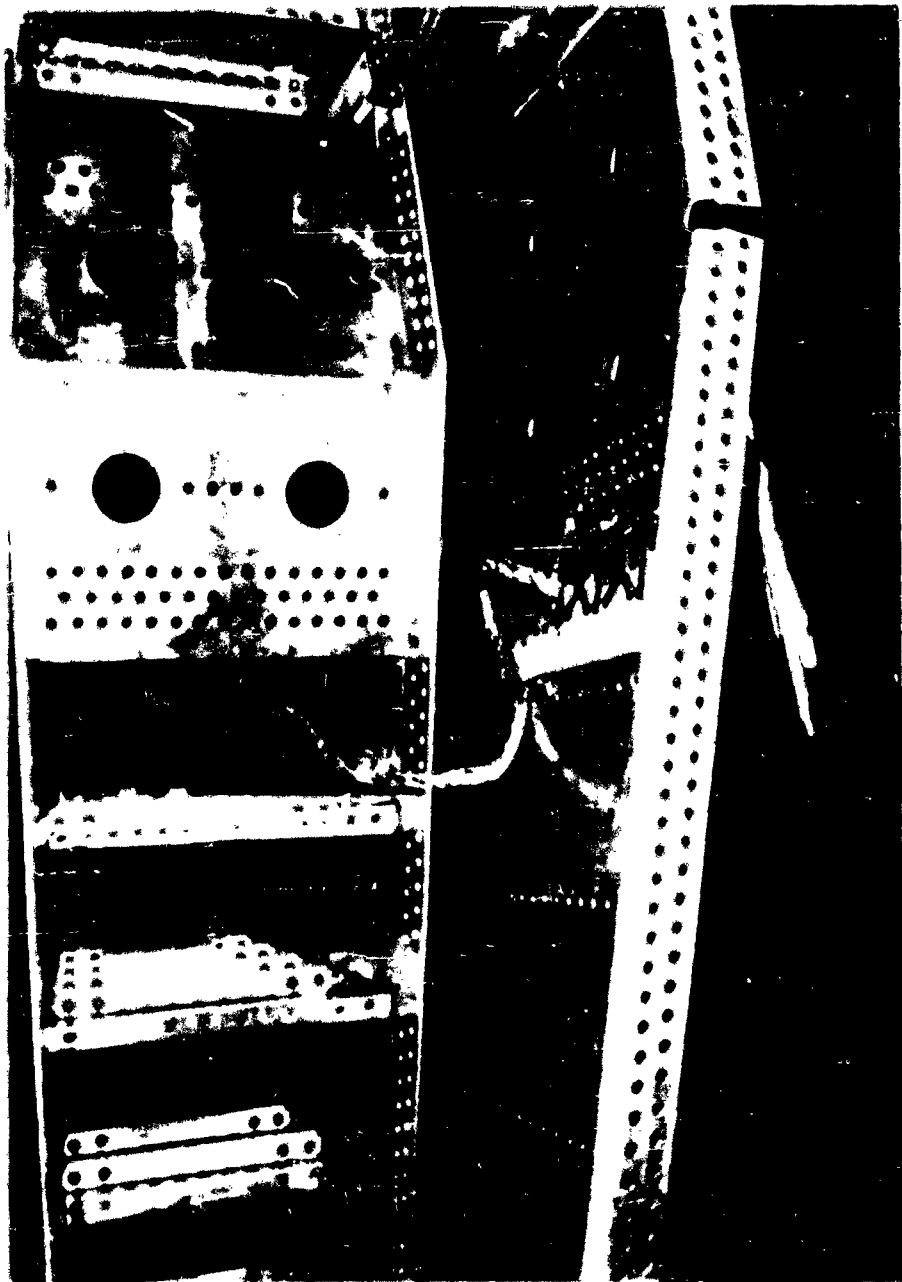


15.128  
Plate 2



DETAILS OF THE INTERNAL CONSTRUCTION OF THE BOX

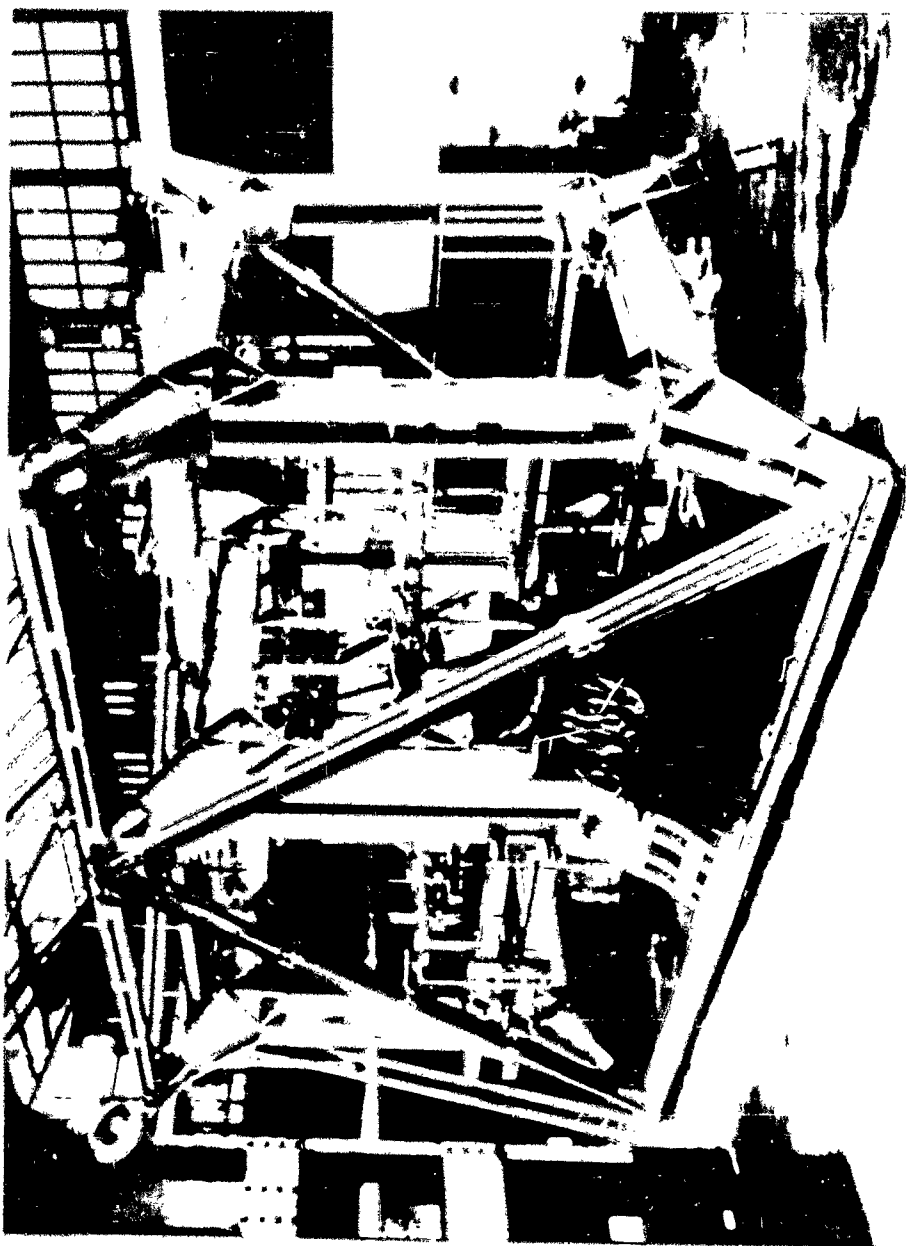
15128  
Page 3

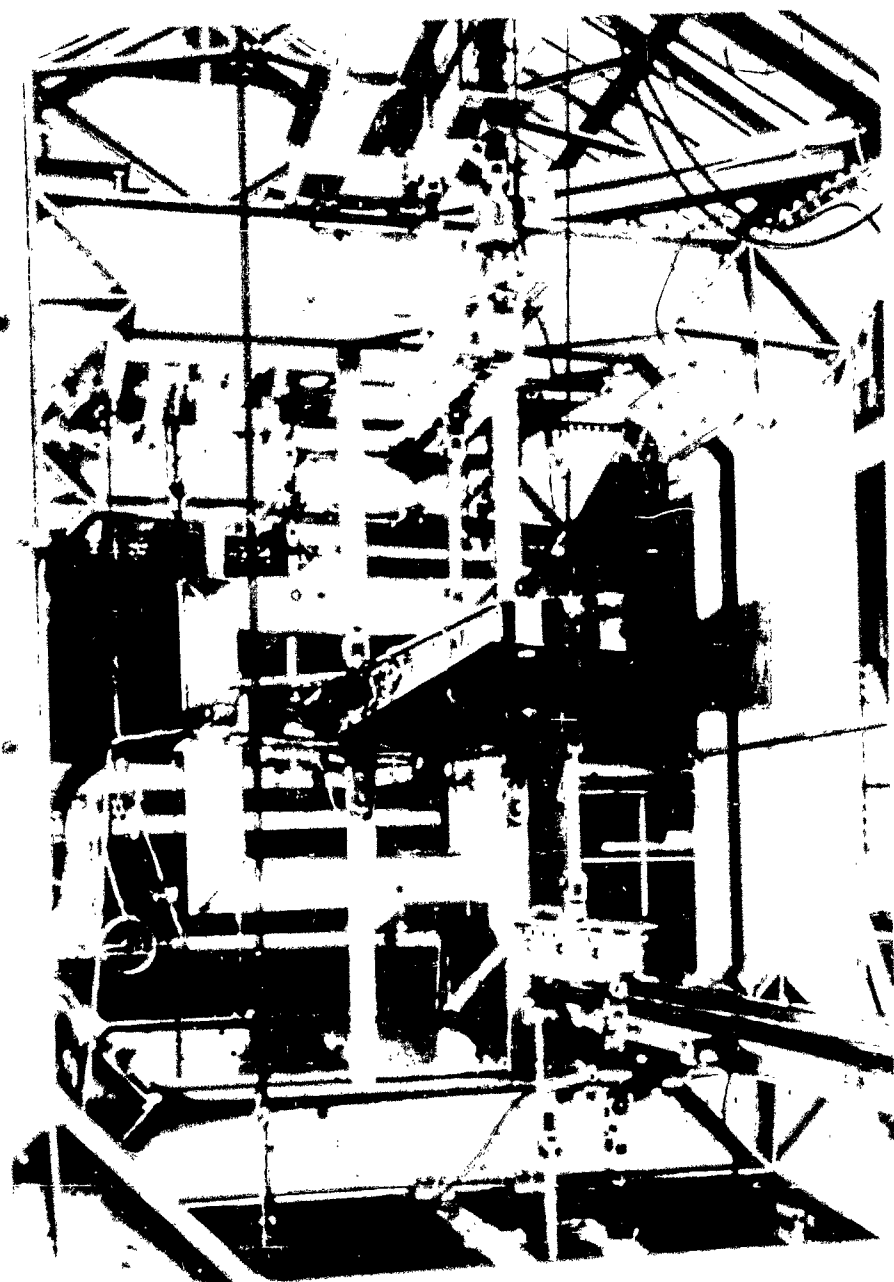


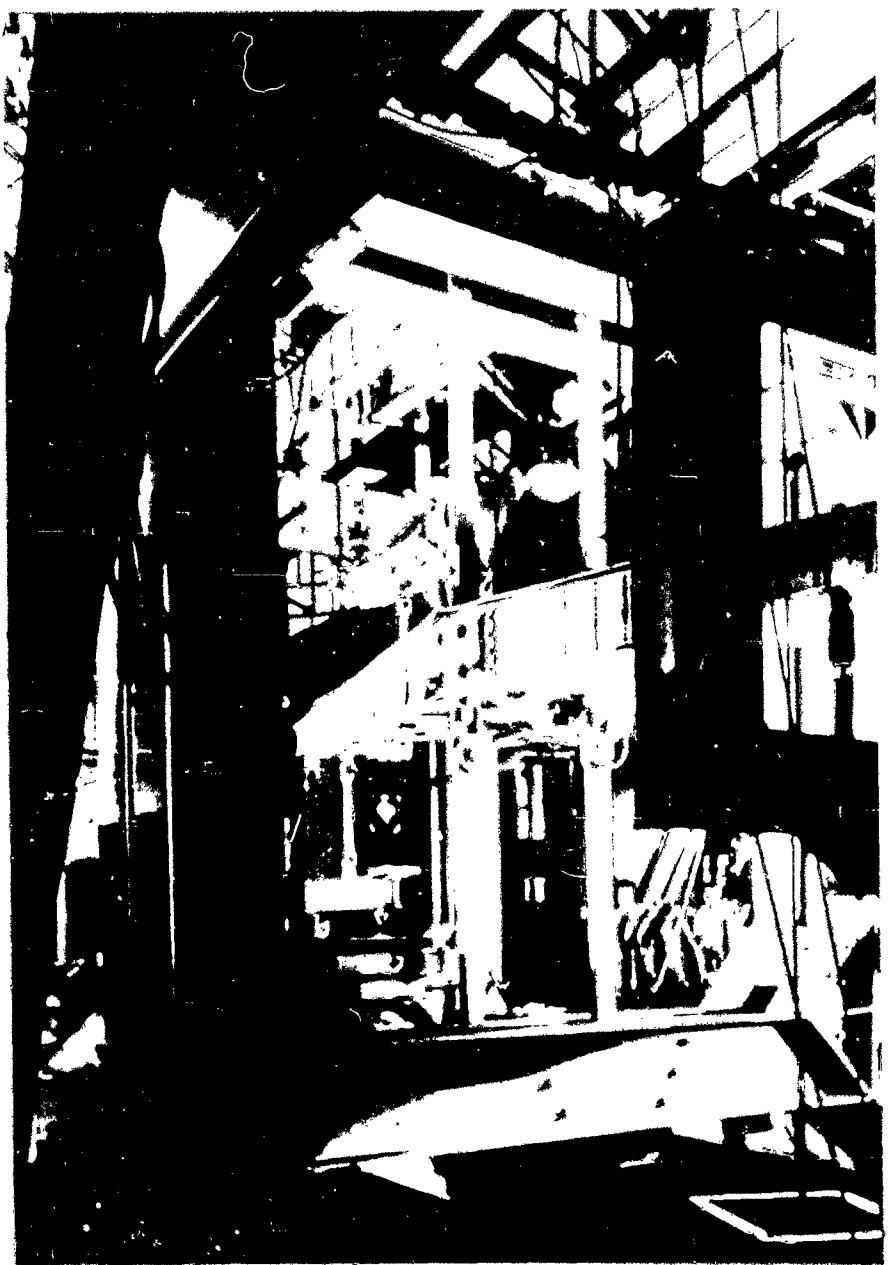
Construction of this Internal Construction of the Box



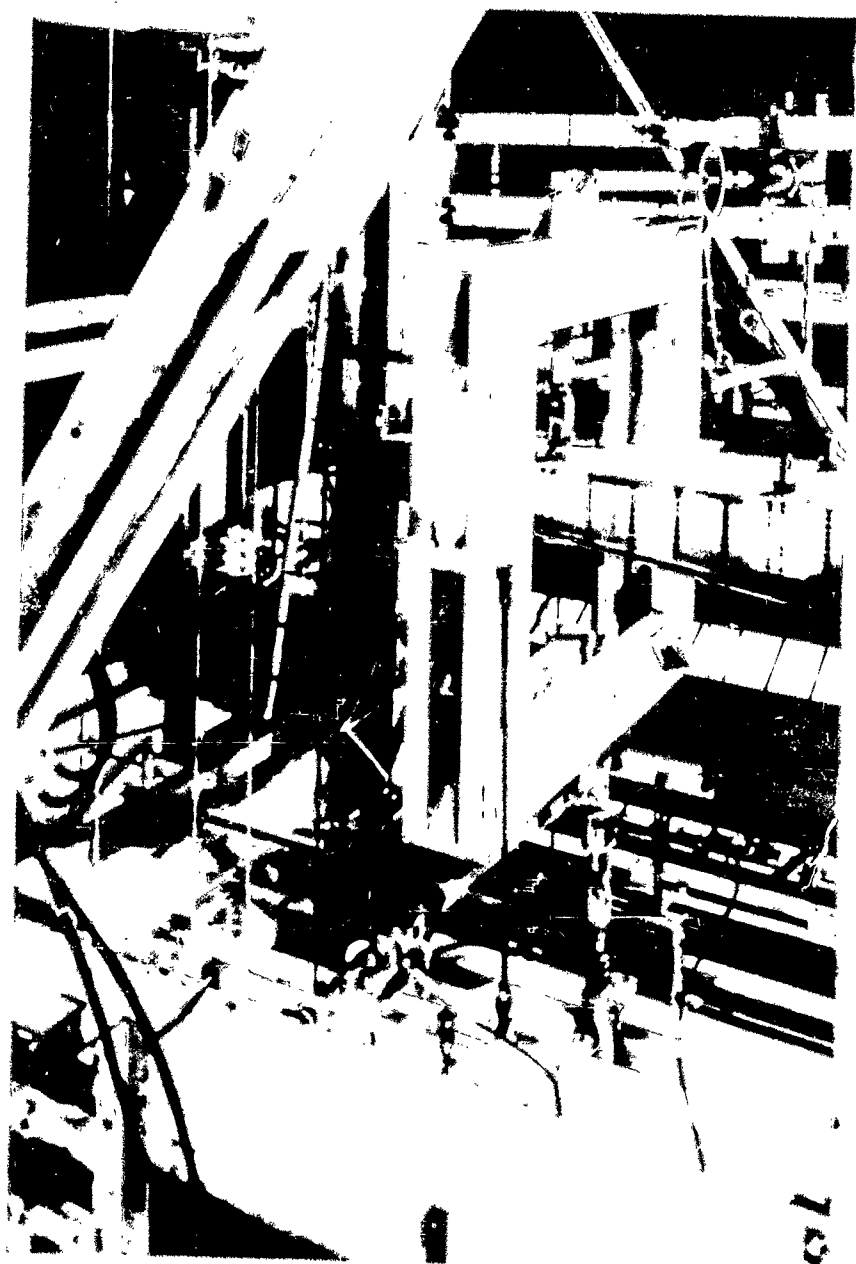
Fig. 1. A photograph of a plant specimen used in the study.



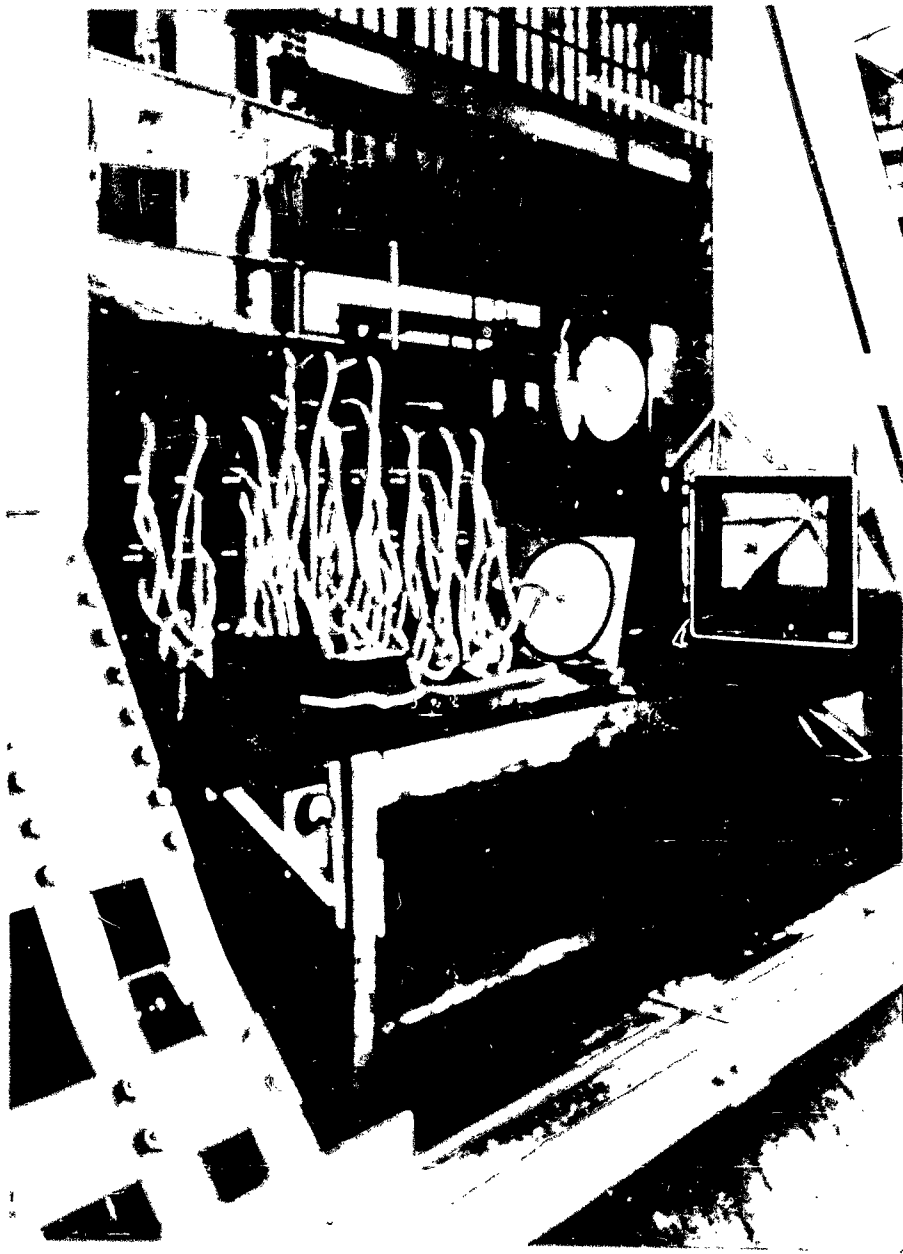




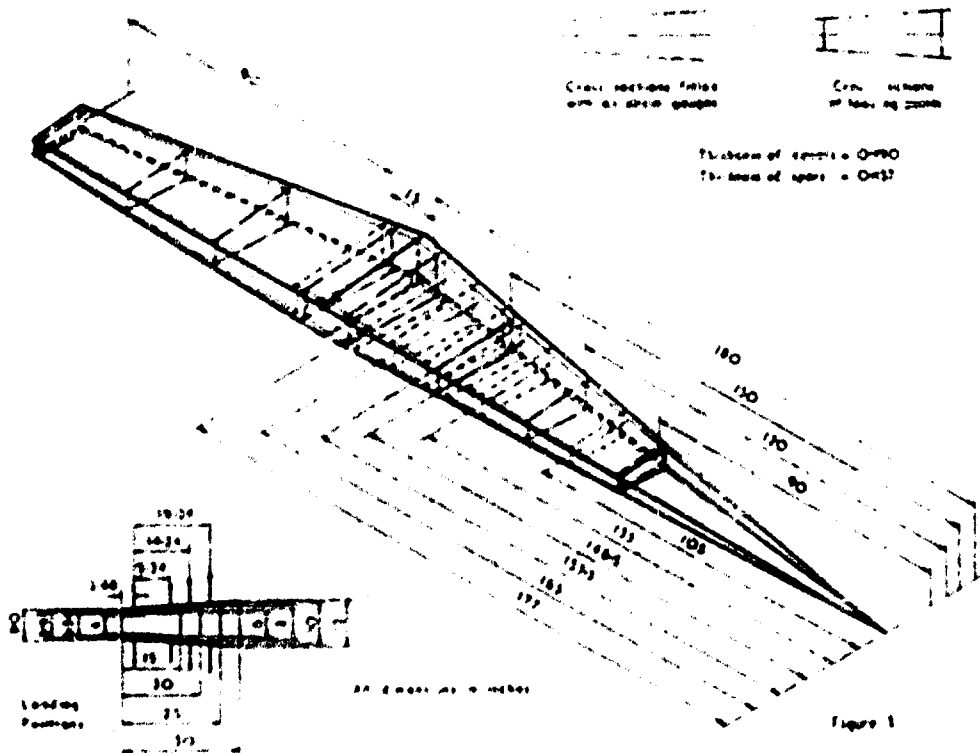
1980-00000000000000000000000000000000



el



19. *Leucosia* — *leucostoma* — *leucostoma*



ISOMETRIC DIAGRAM OF THE FORWARD CAR

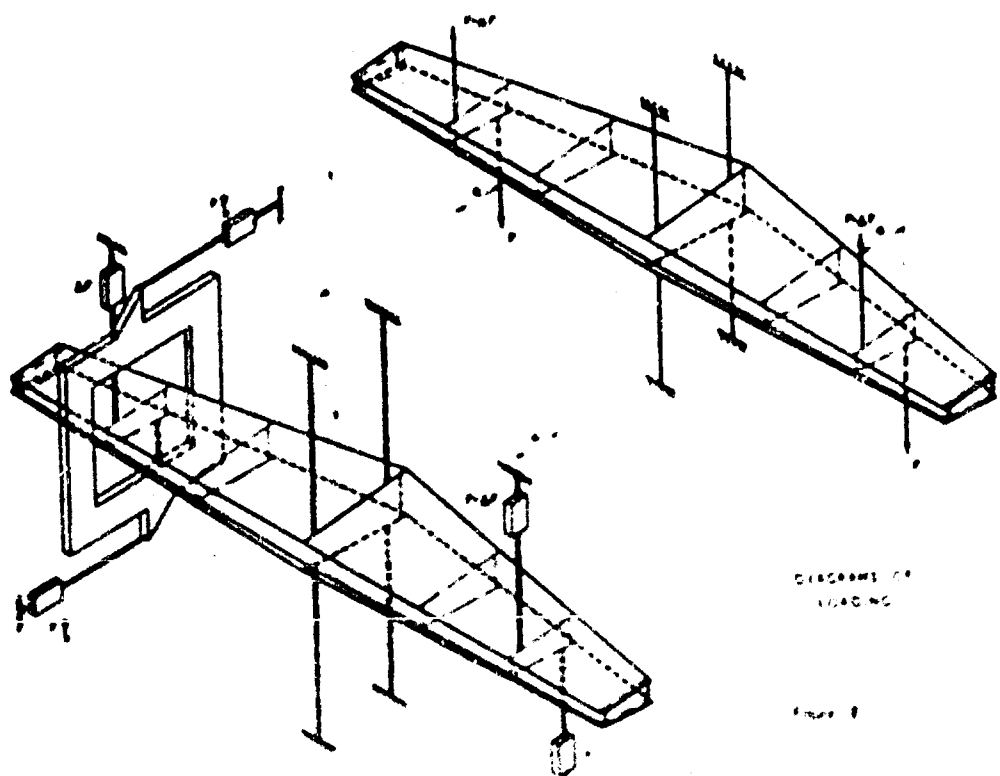
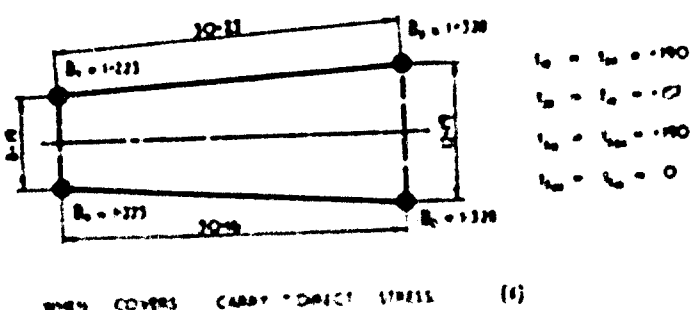
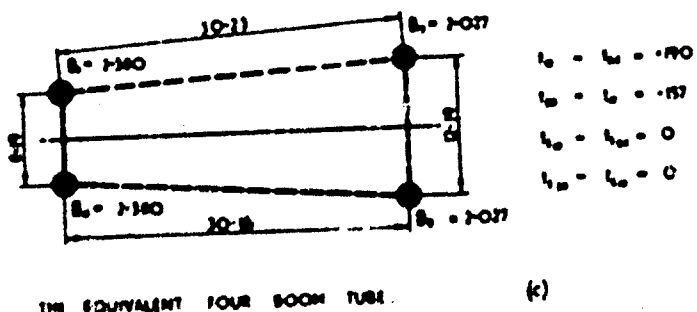
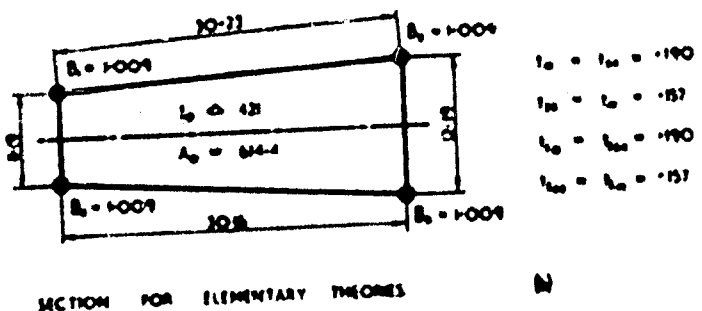
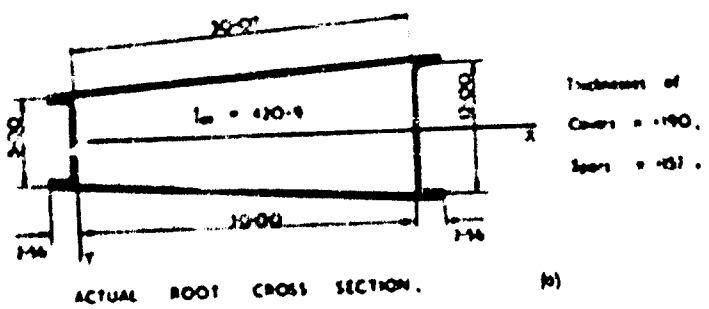
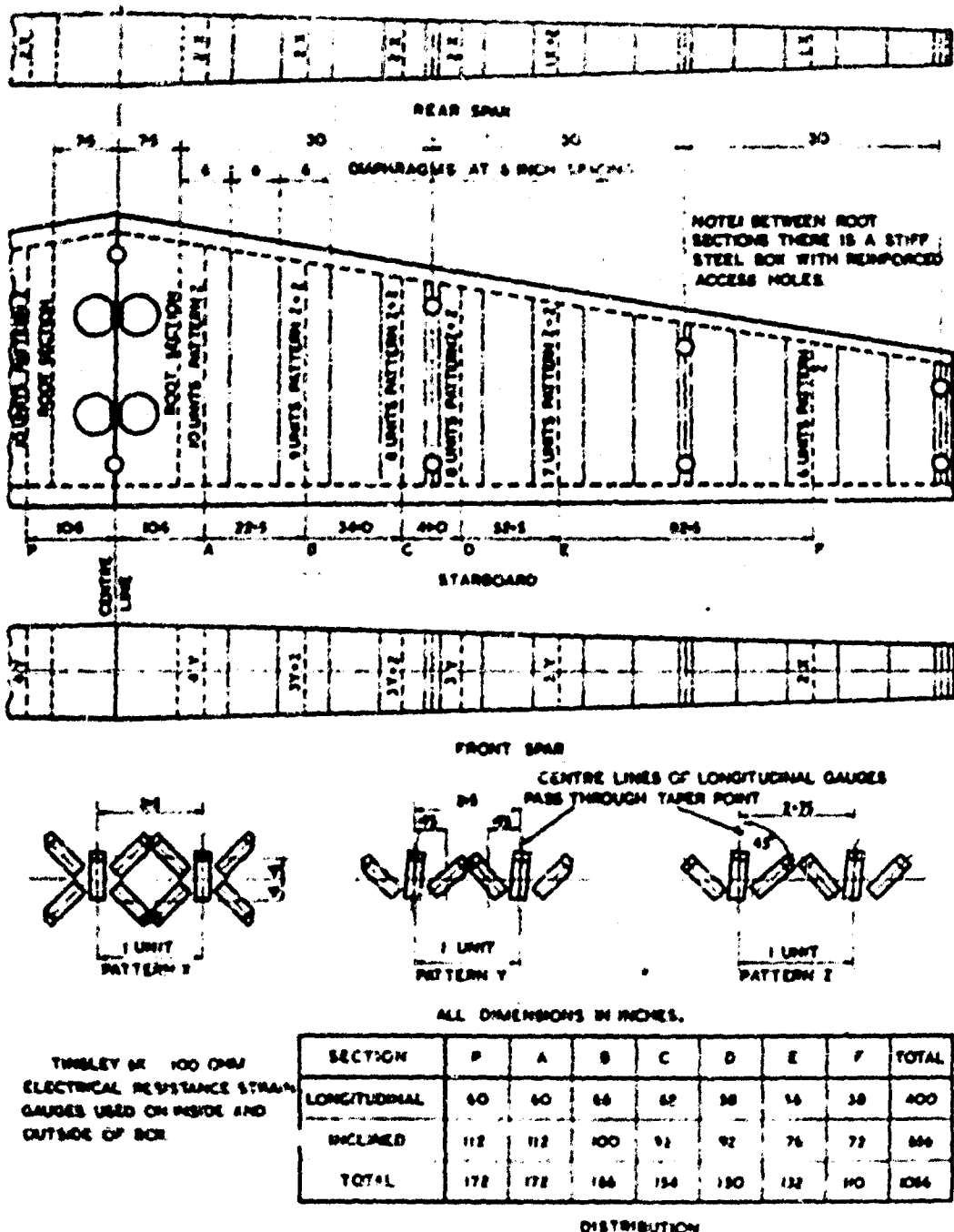


Figure 2



ROOT CROSS SECTION DIMENSIONS USED IN COMPUTATION  
(All dimensions in meters) Figure 3.

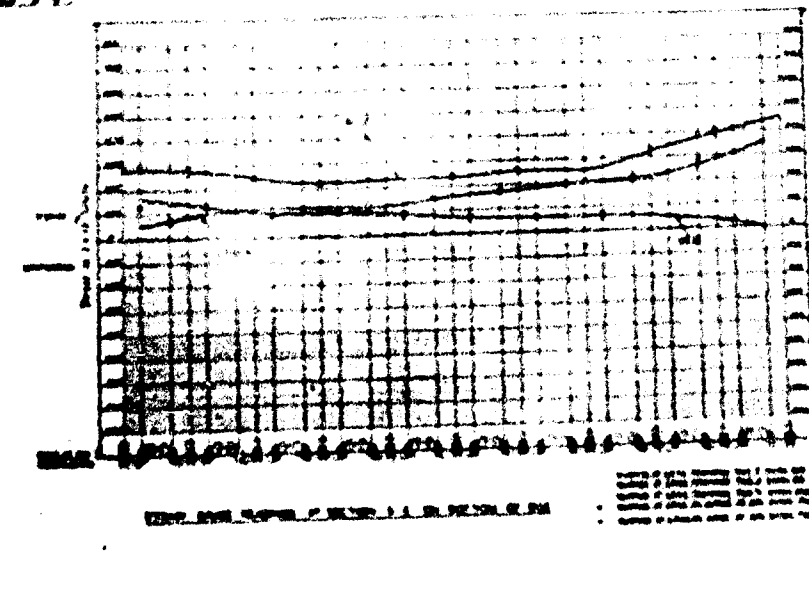


ARRANGEMENT OF STRAIN GAUGES FOR TAPERED BOX.

Figure 4

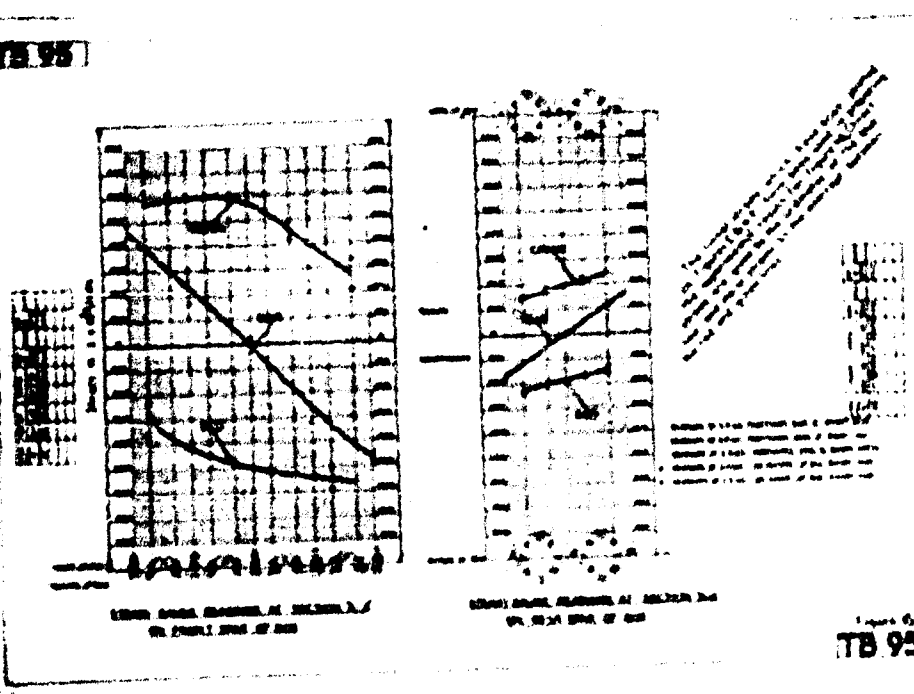
THIRLEY OR 100 OHM  
ELECTRICAL RESISTANCE STRAIN  
GAUGES USED ON INSIDE AND  
OUTSIDE OF BOX.

TB94



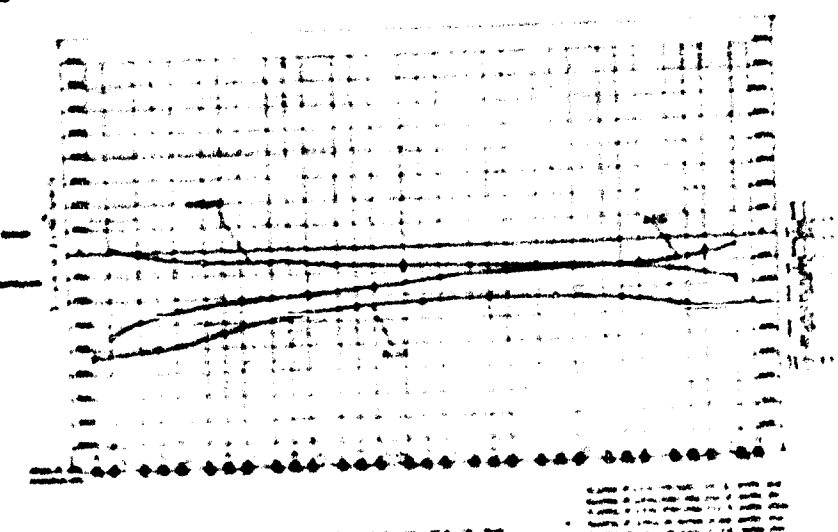
TB94

TB95

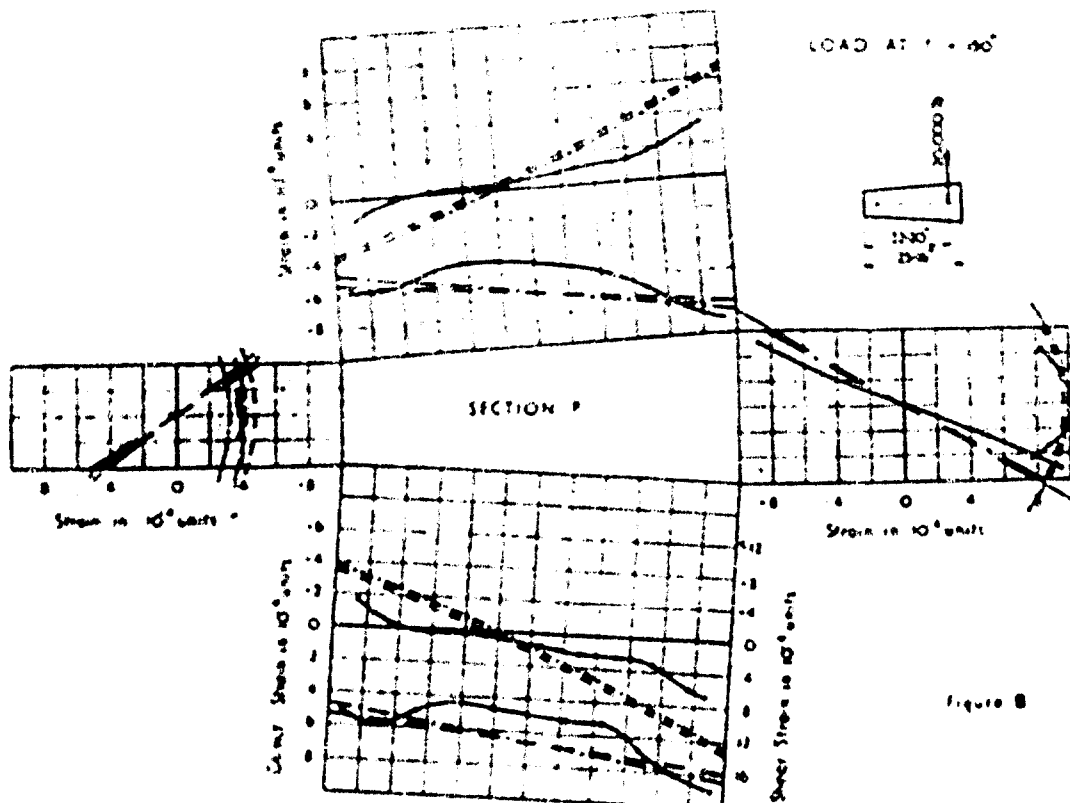


TB95

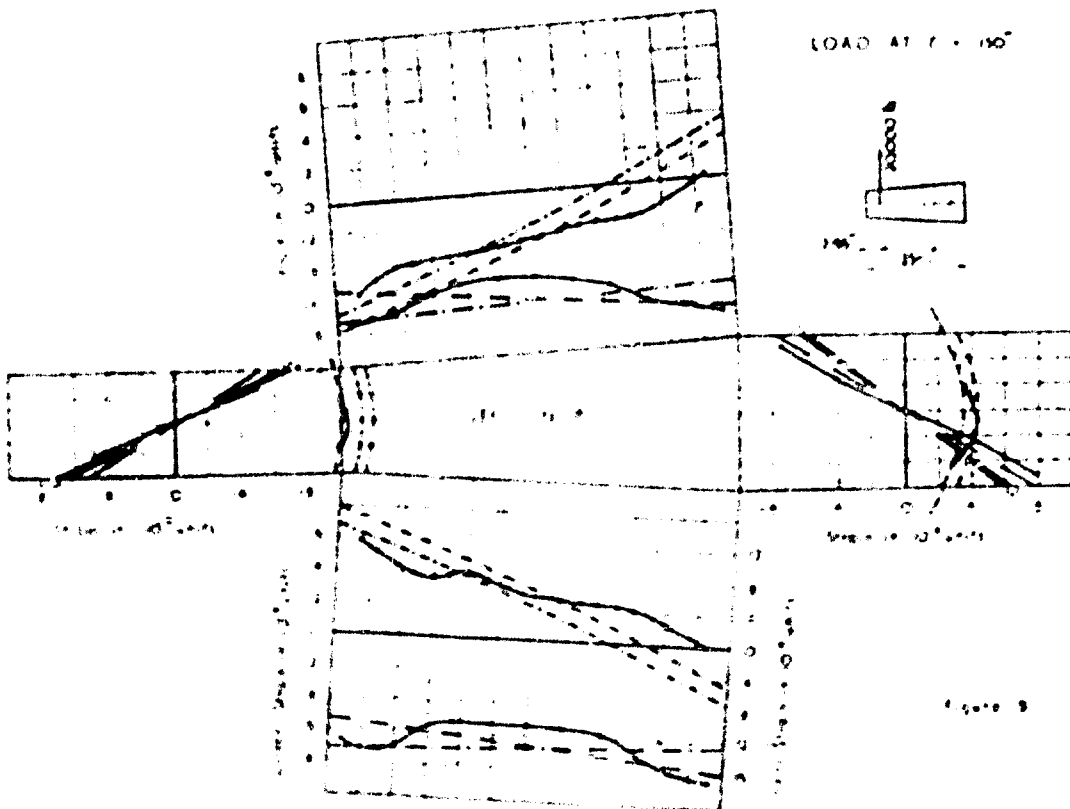
TB93



TB93



	Direct Strain	Shear Strain	
Experiment	—	—	Tensile girder and anticlockwise shear strains are considered positive and are plotted outwards.
Geometry Theory	— — —	— — —	The direct strains are drawn full scale and the shear strains half scale.
Equivalent four beam tube	— — —	— — —	
Covers carrying direct strain	— — —	— — —	



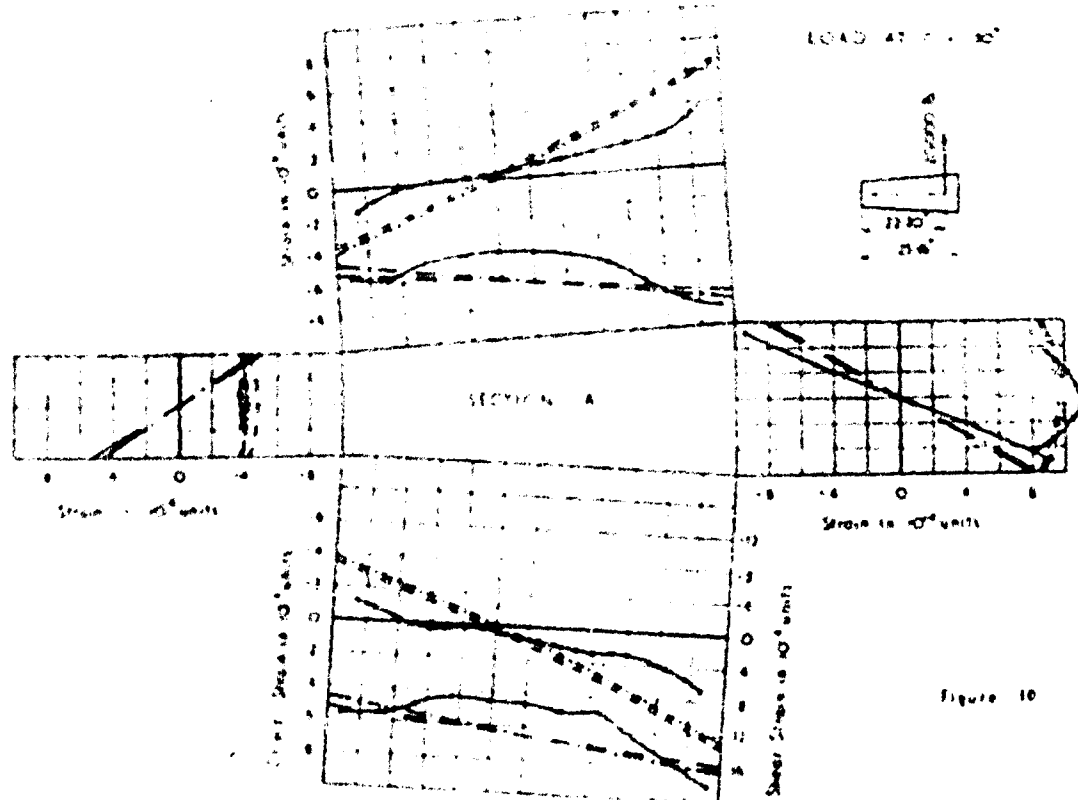


Figure 10

Type	Strain	Shear	Strain
Elementary Shear	—	—	—
Elementary Four from base	—	—	—

Tensile strains and compressive shear strains are considered positive and are plotted outwards. The direct shear are drawn full scale and the shear strains half scale.

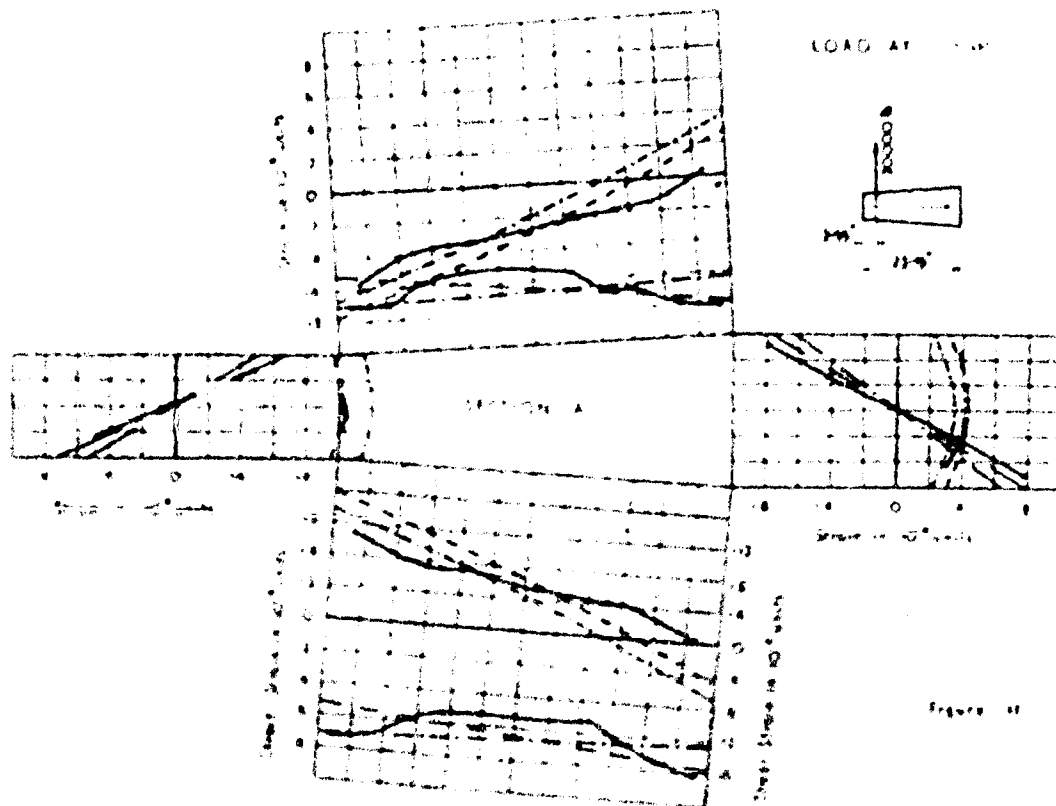


Figure 11

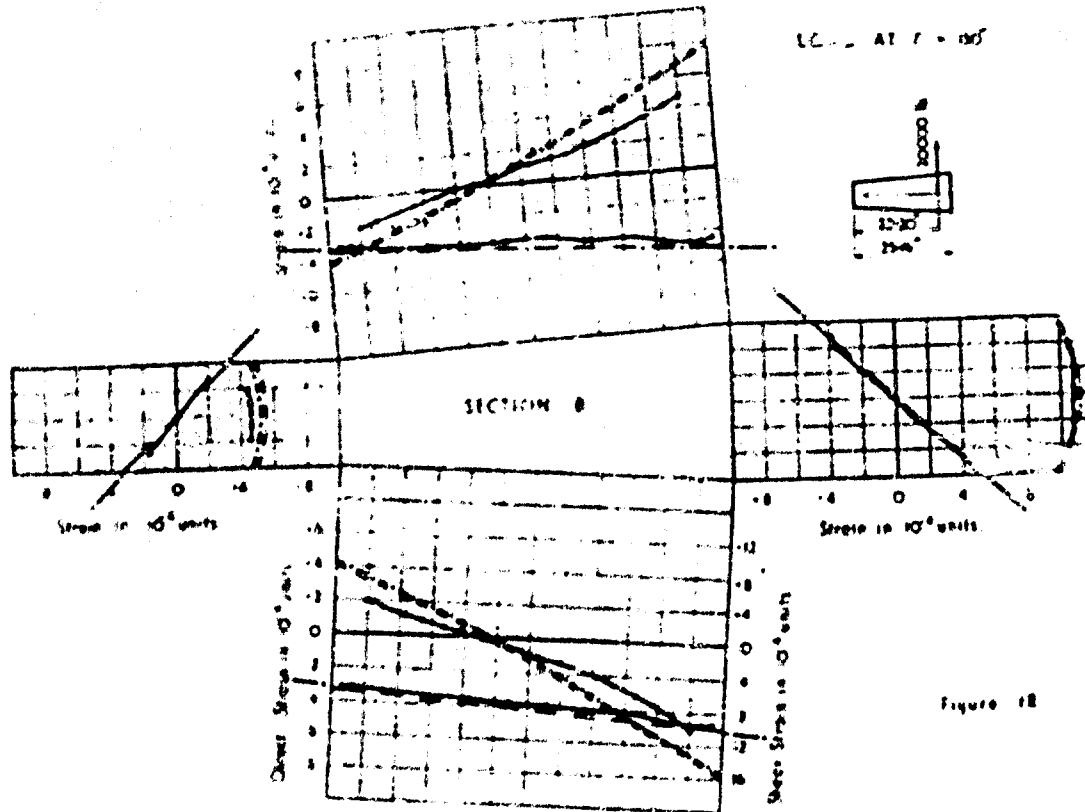


Figure 18

	Direct Shear	Shear Stress
Experimental	—	—
Hencky's Theory	---	—
Tresca's Theory	----	-----

Tensile stresses and compressive shear stresses are considered positive and are plotted outwards. The direct stresses are drawn full scale and the shear stresses half scale.

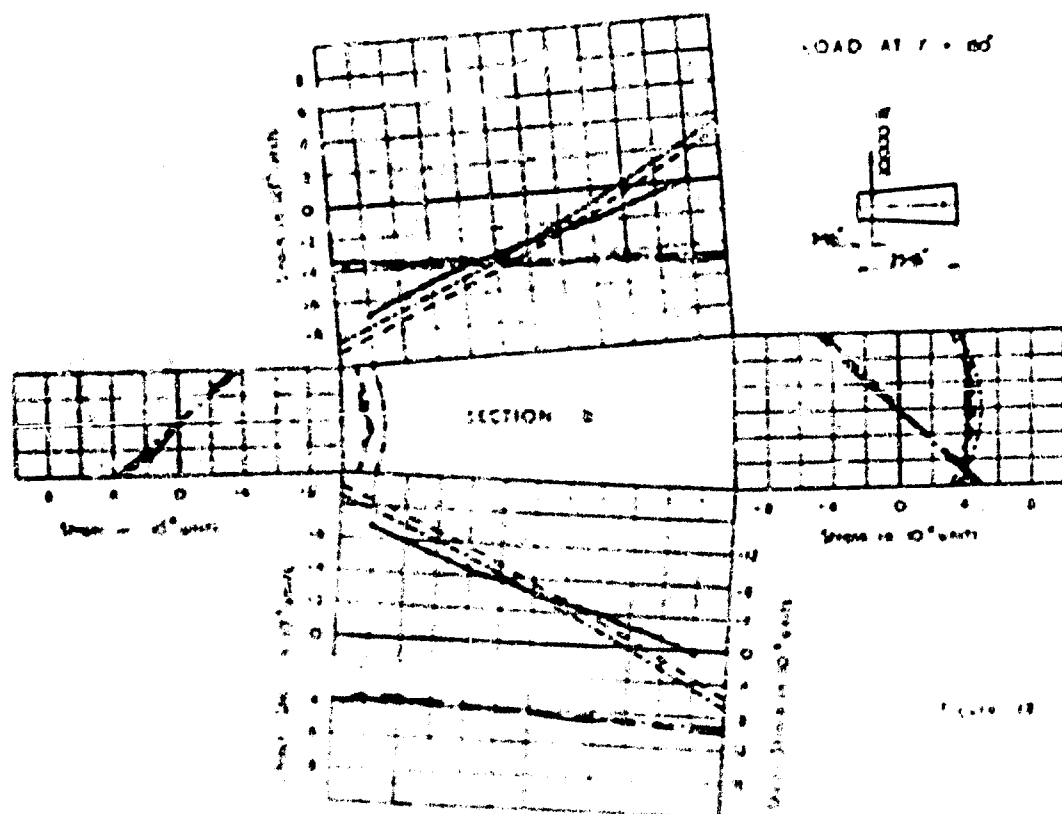


Figure 19

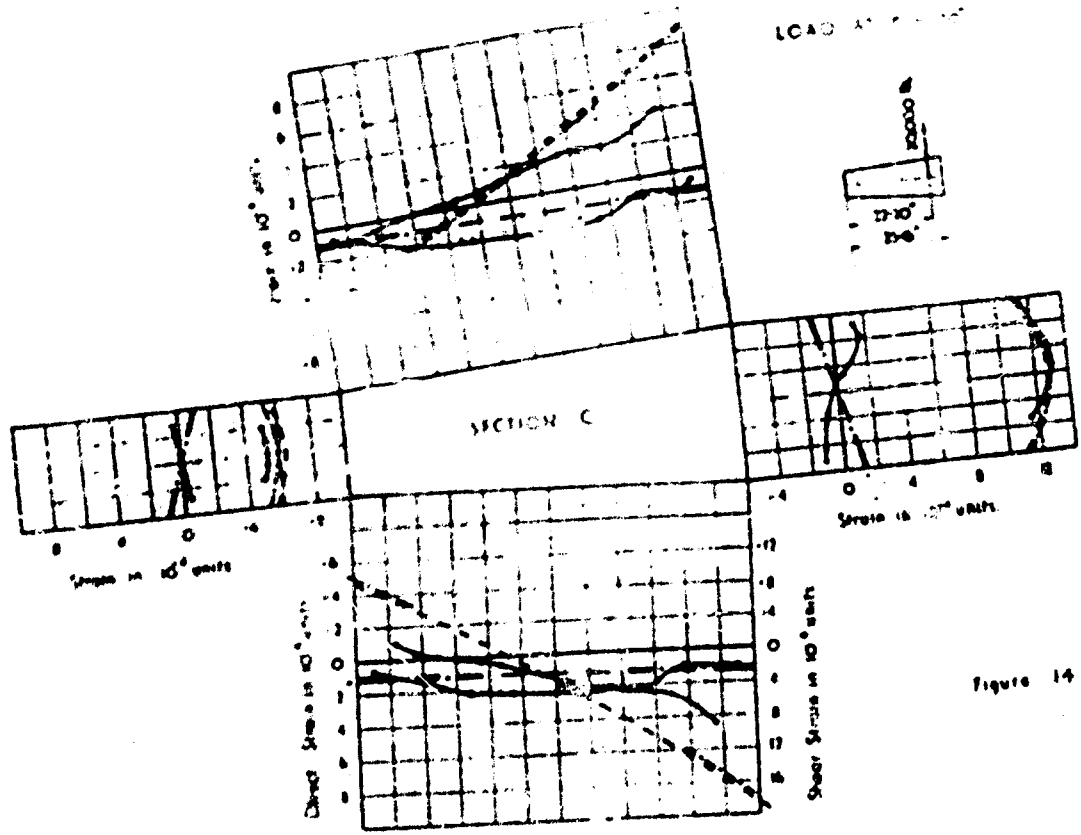


Figure 14

Experiment  
Elementary Theory  
Torsion for  
beam tube

Direct Stress	Shear Stress
—	—
---	- - -
- - -	- - - -

Torsion stress and non-torsion shear stresses are considered positive and are plotted outward. The direct stress are drawn full scale and the shear stresses half scale.

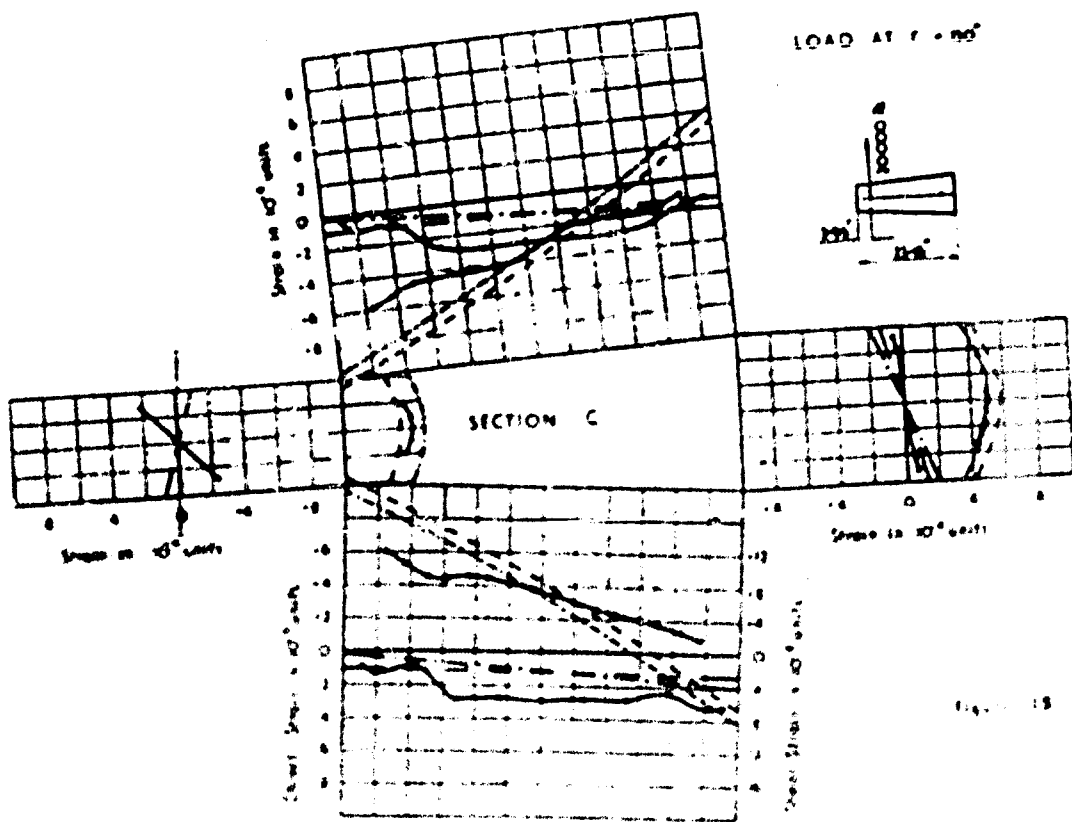
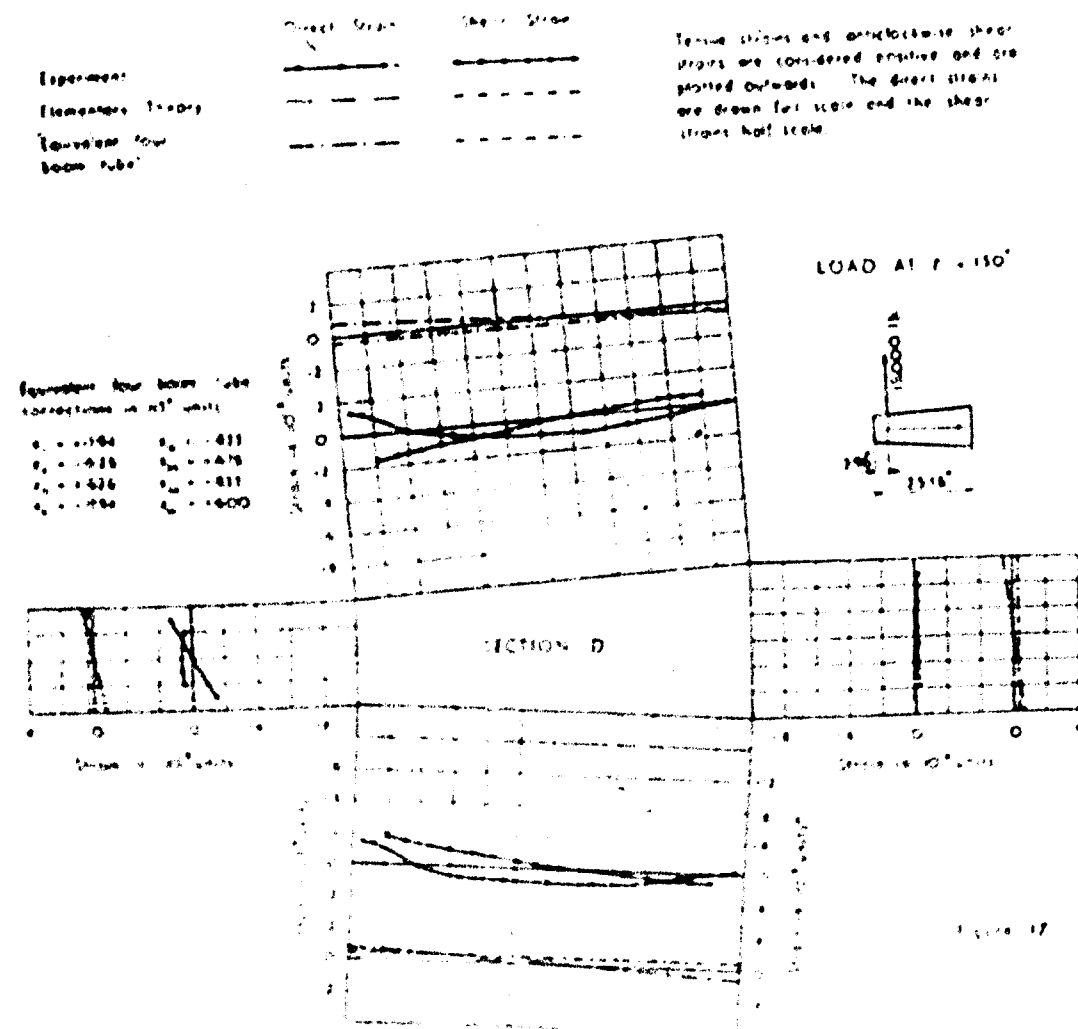
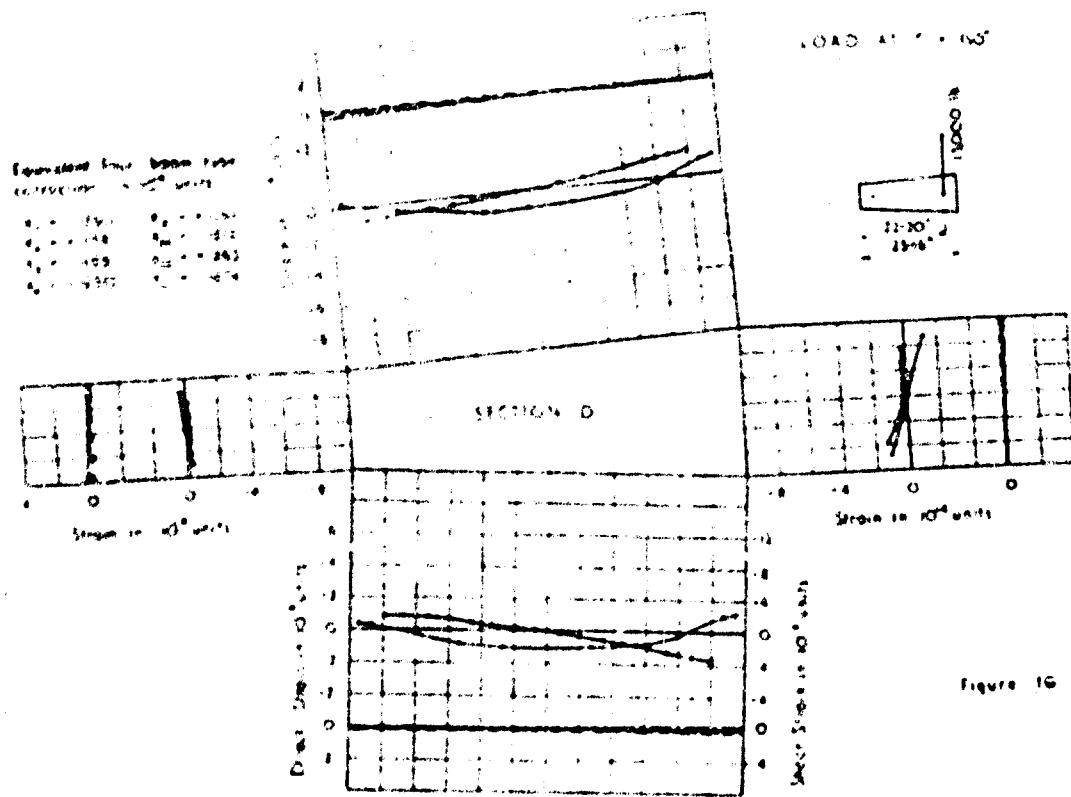
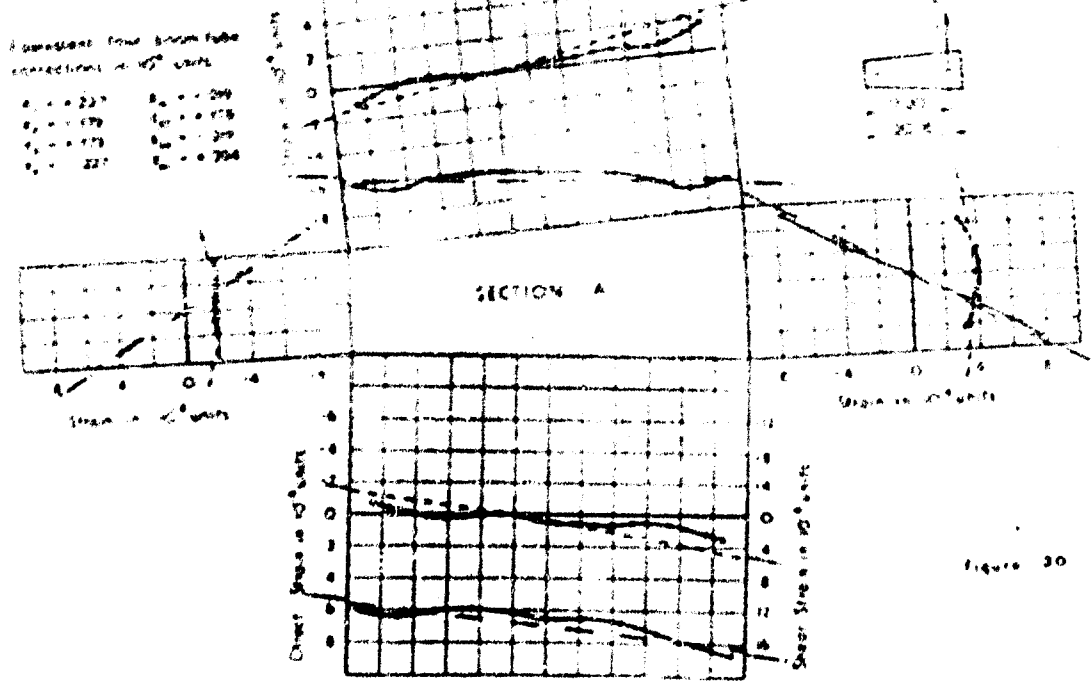


Figure 15

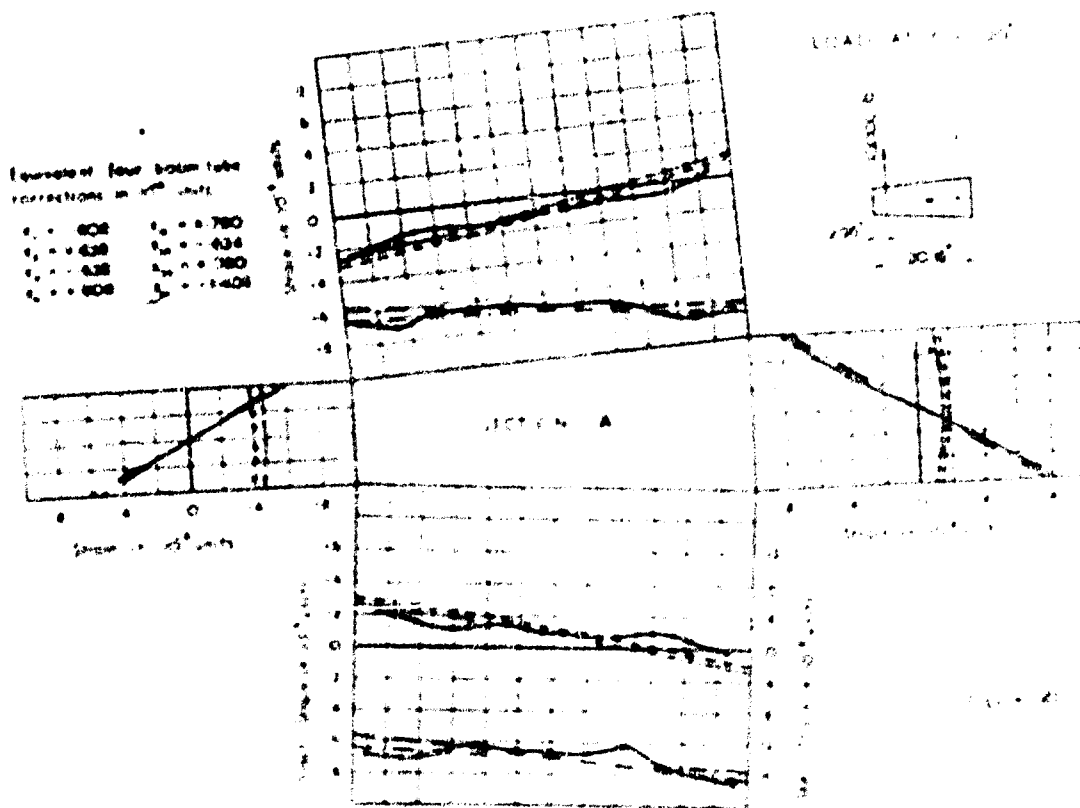




Legend:

	Direct Strain	Shear Strain
Experiment	—	—
Elementary Theory	—	—
Equivalent four beam tube	—	—

Normal strains and shear strains. These plots are considered positive and are plotted outwards. The 0-12 lines are drawn full scale and the strain plots half scale.



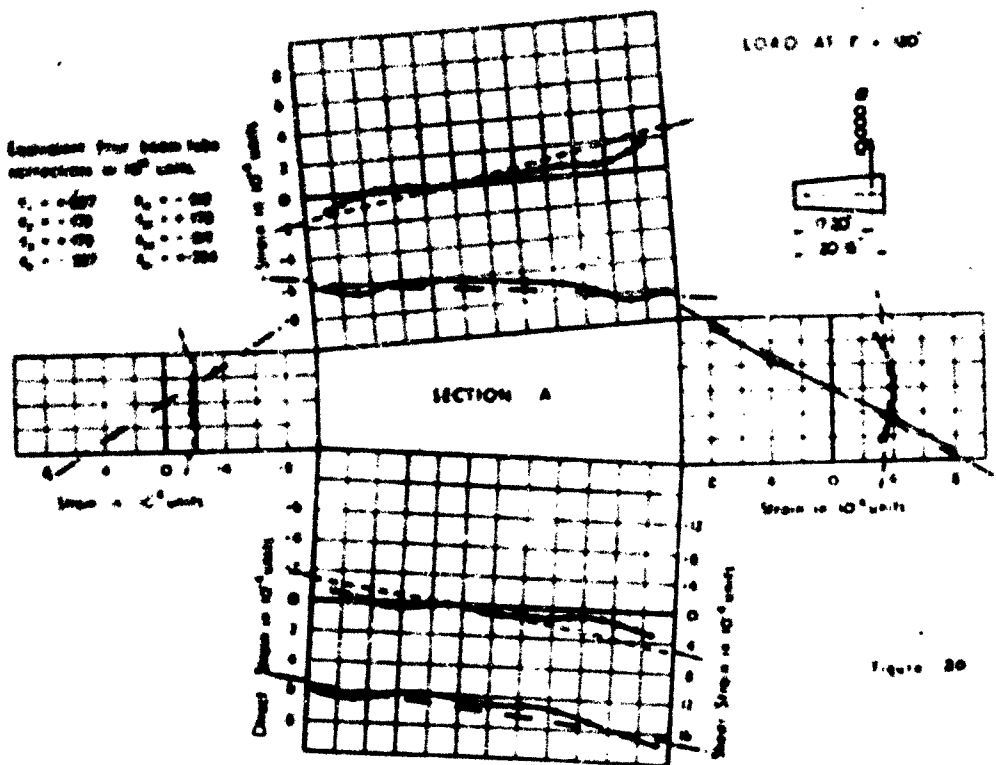


Figure 20

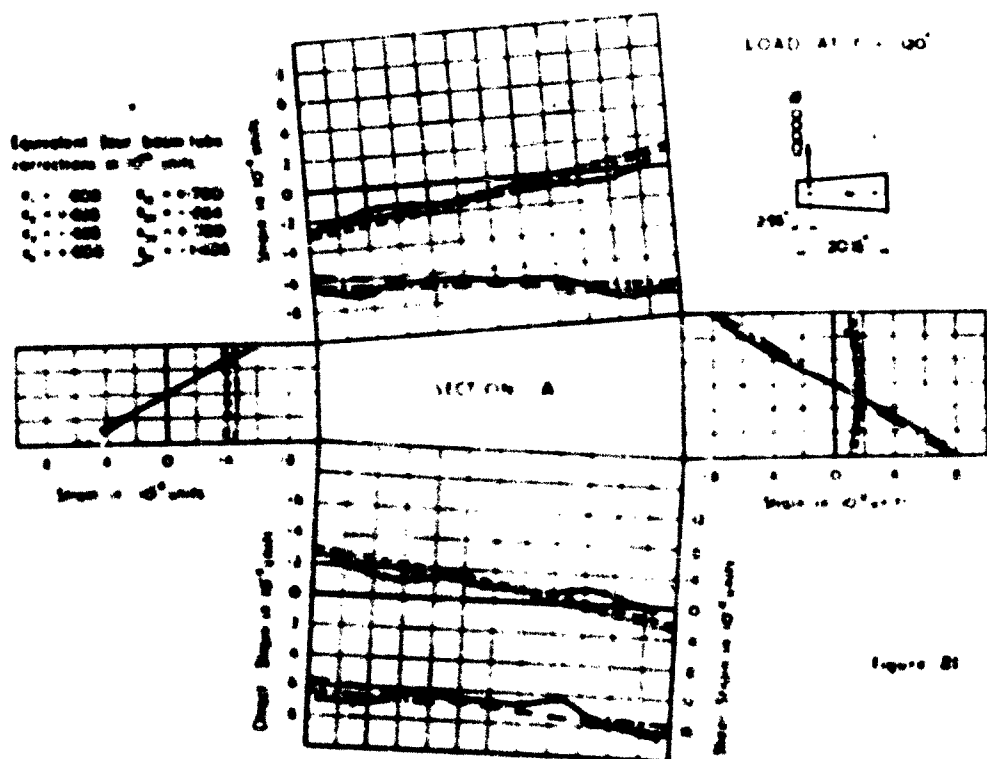
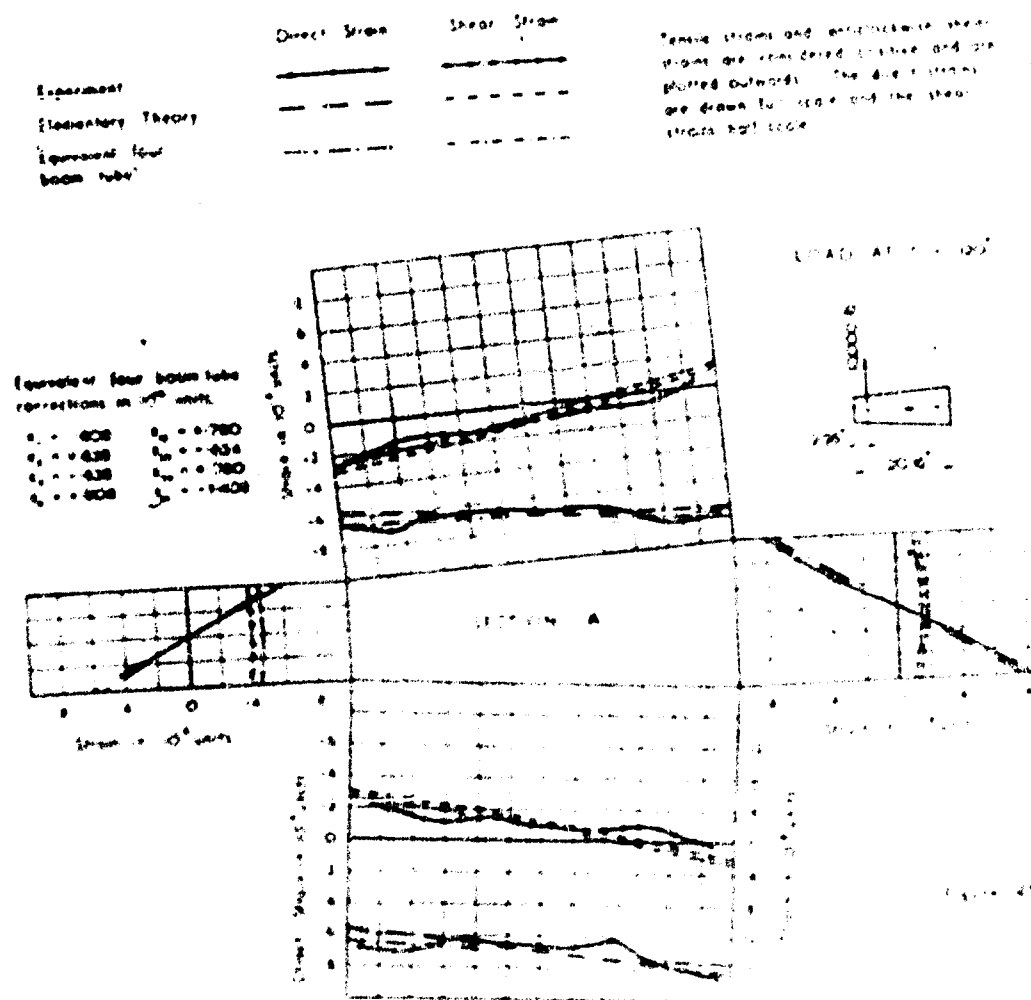
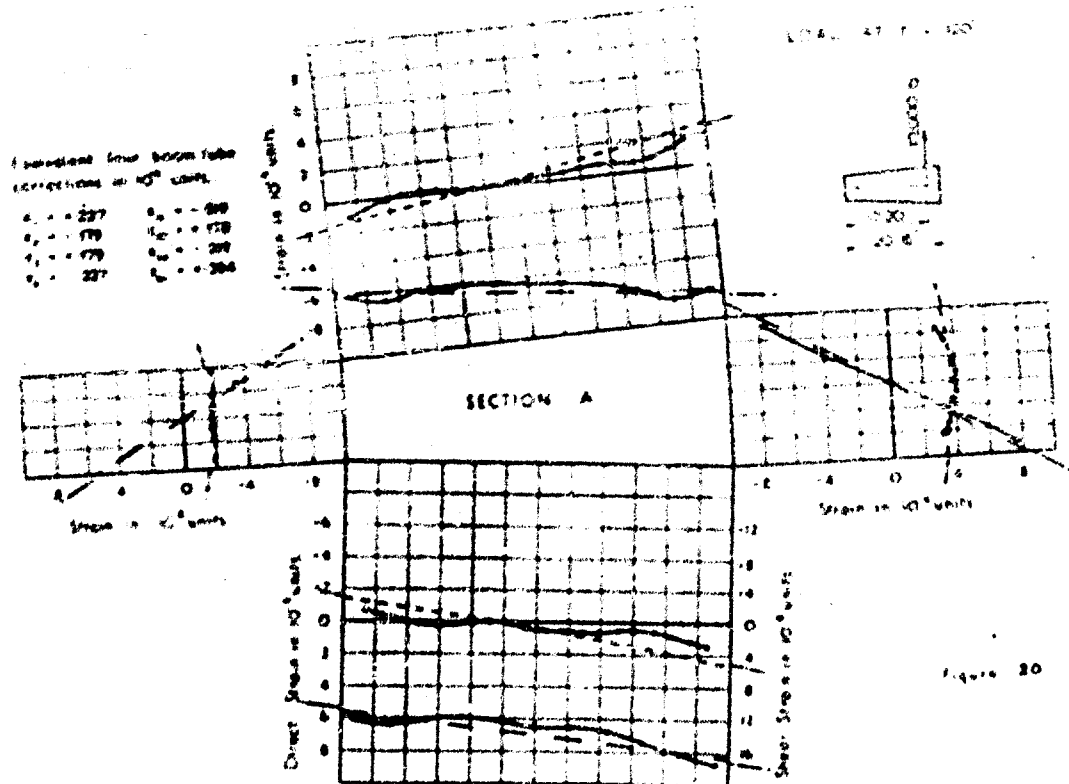
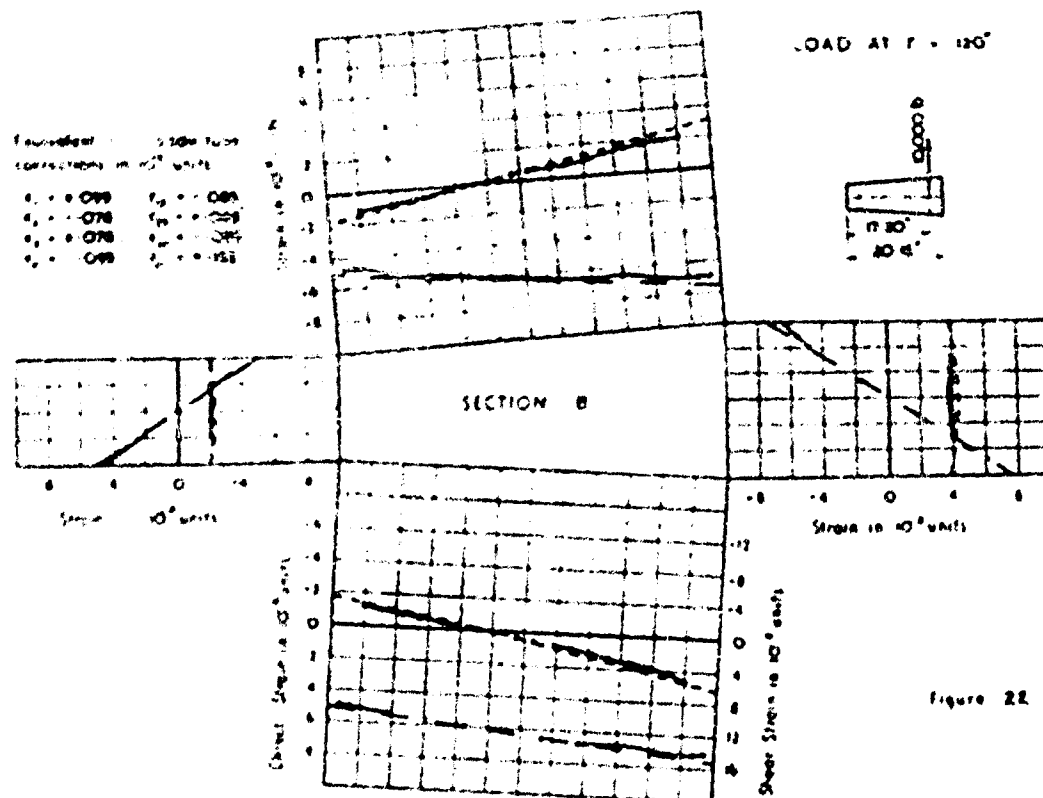


Figure 21

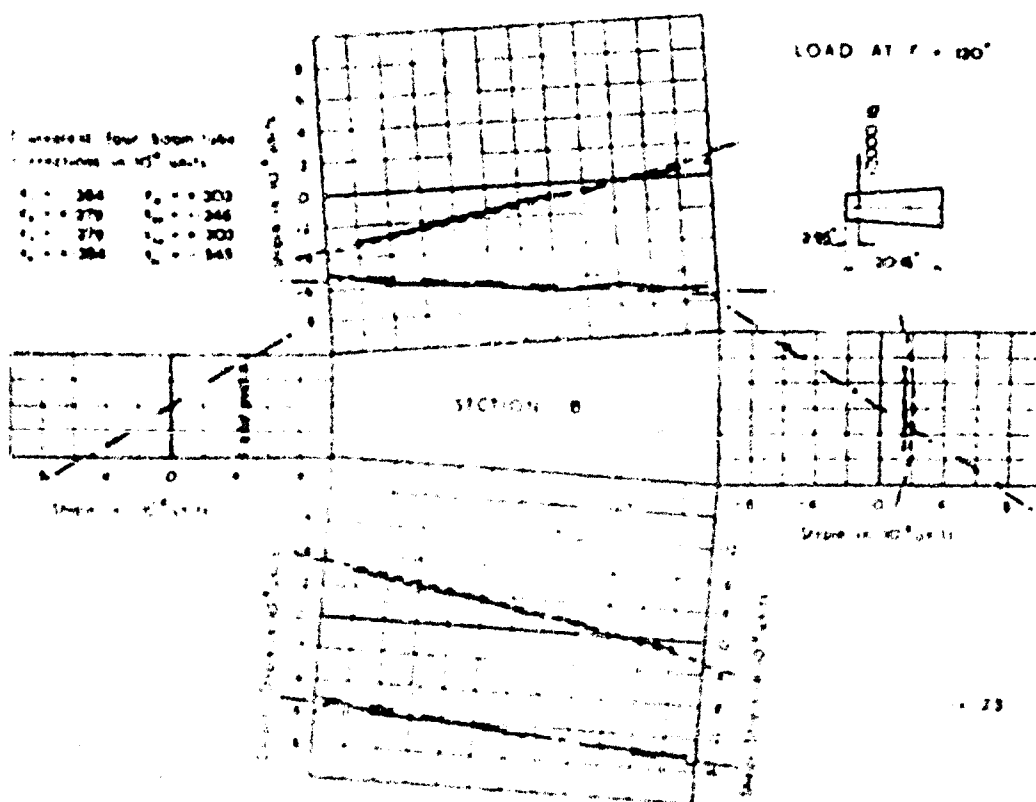


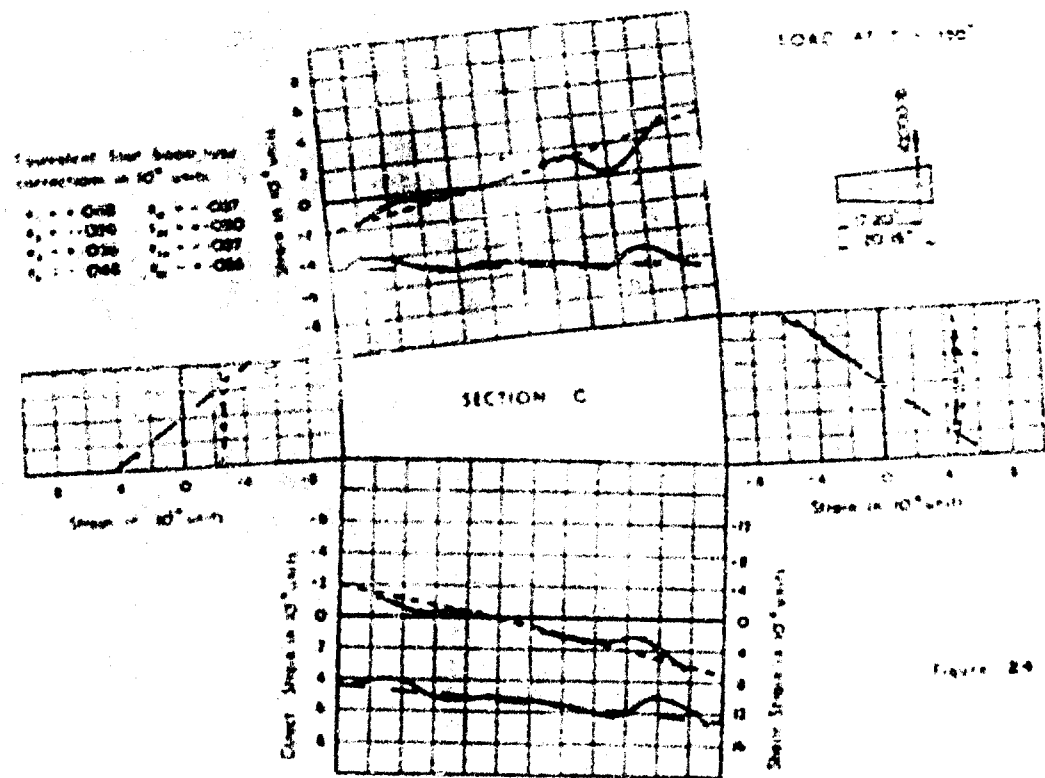


Shear Stress      Shear Strain

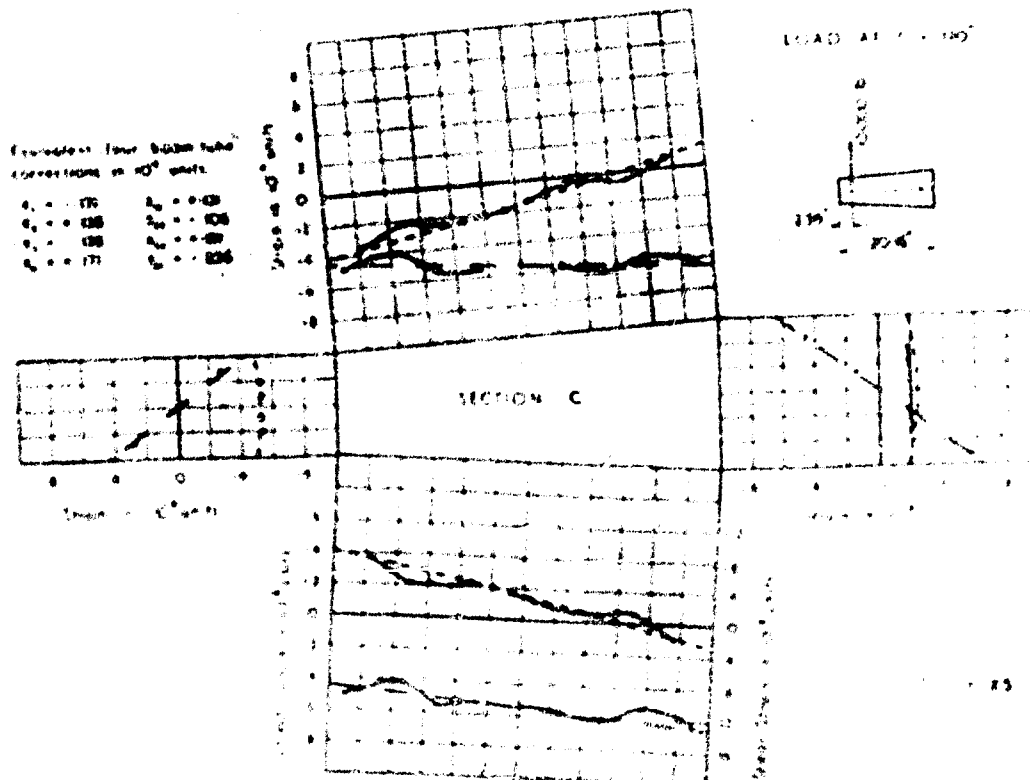
Experiment	—	—
Holmberg, Theory	—	—
Four-beam tube	—	—

Tensile strains and clockwise shear strains are considered positive and are plotted outwards. The direct strains are drawn full scale and the shear strains half scale.





	Direct Stress	Shear Stress	
Experimental	—	—	Tensile strains and conductance shear strains are considered positive and are plotted upwards. The direct strains are drawn full scale and the shear strains half scale.
Theory	- - -	- - -	



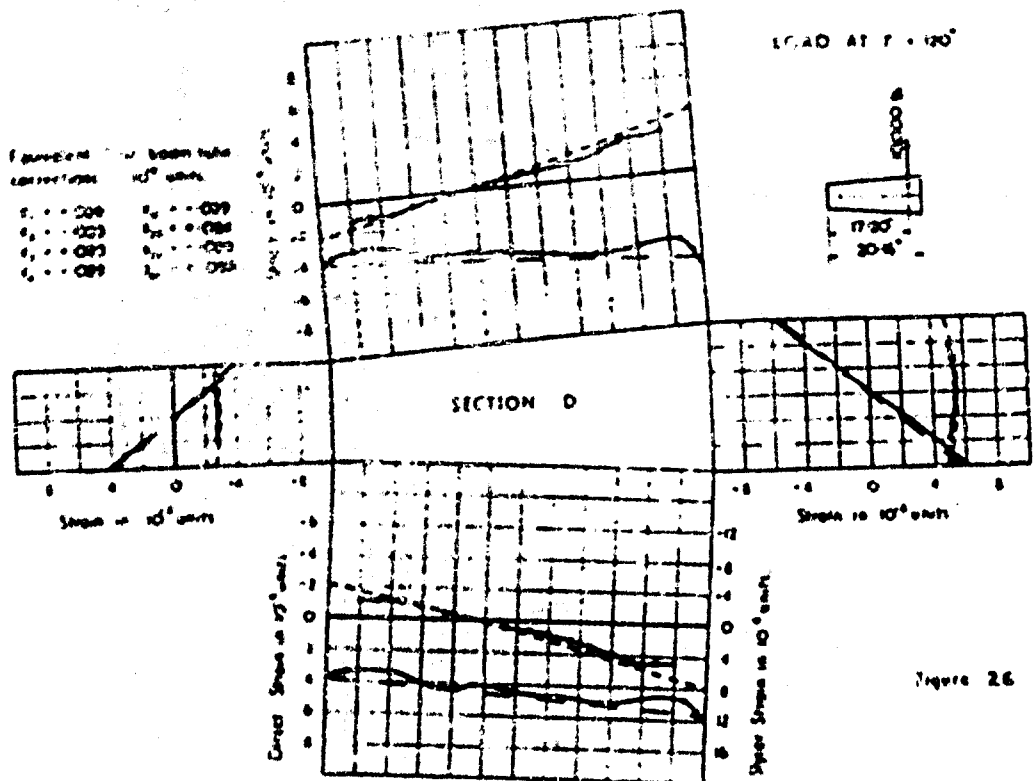


Figure 26

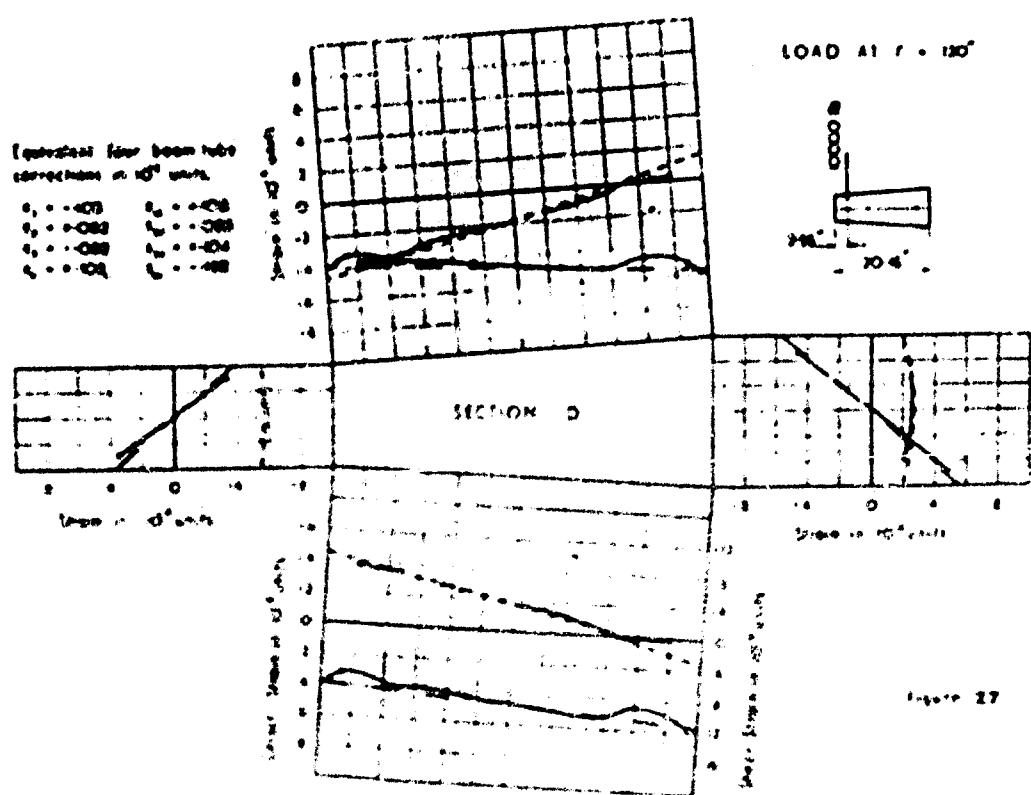
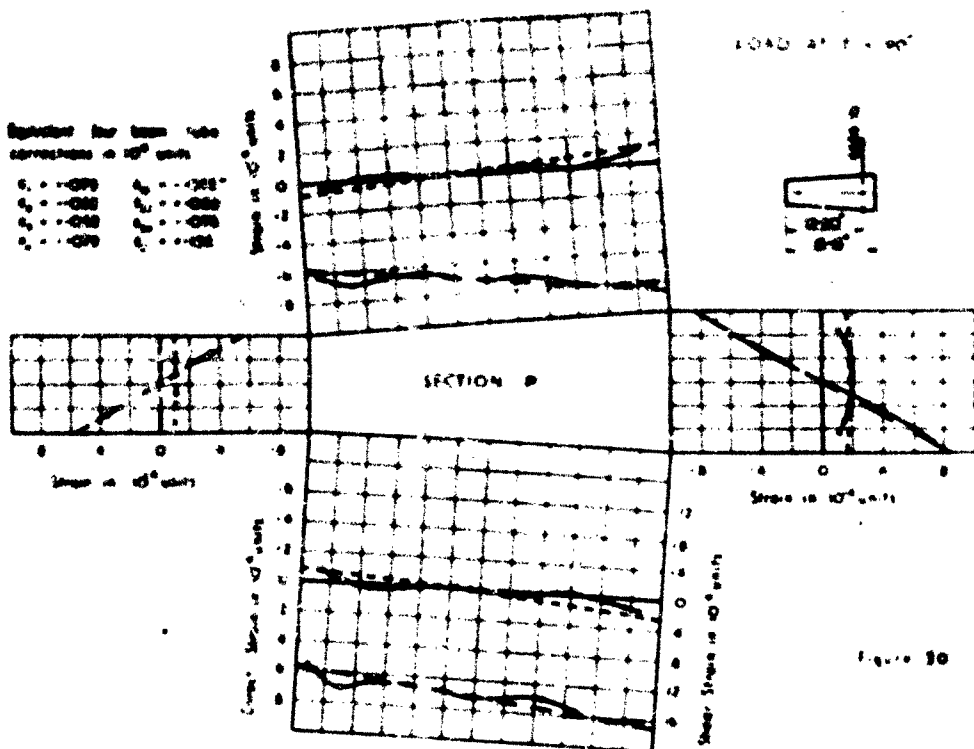
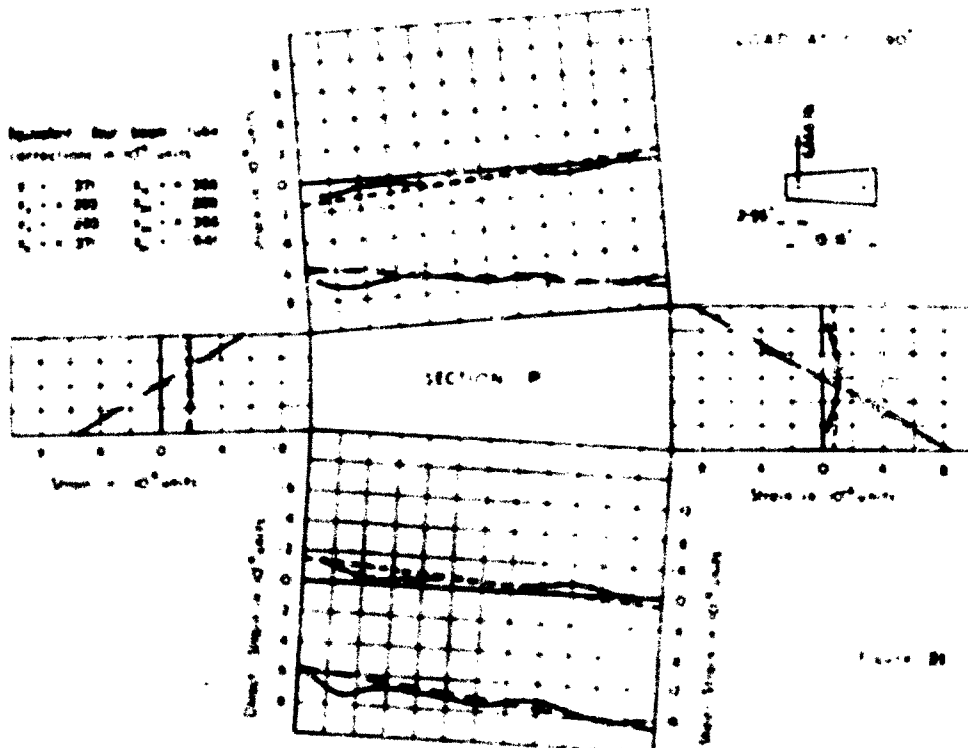
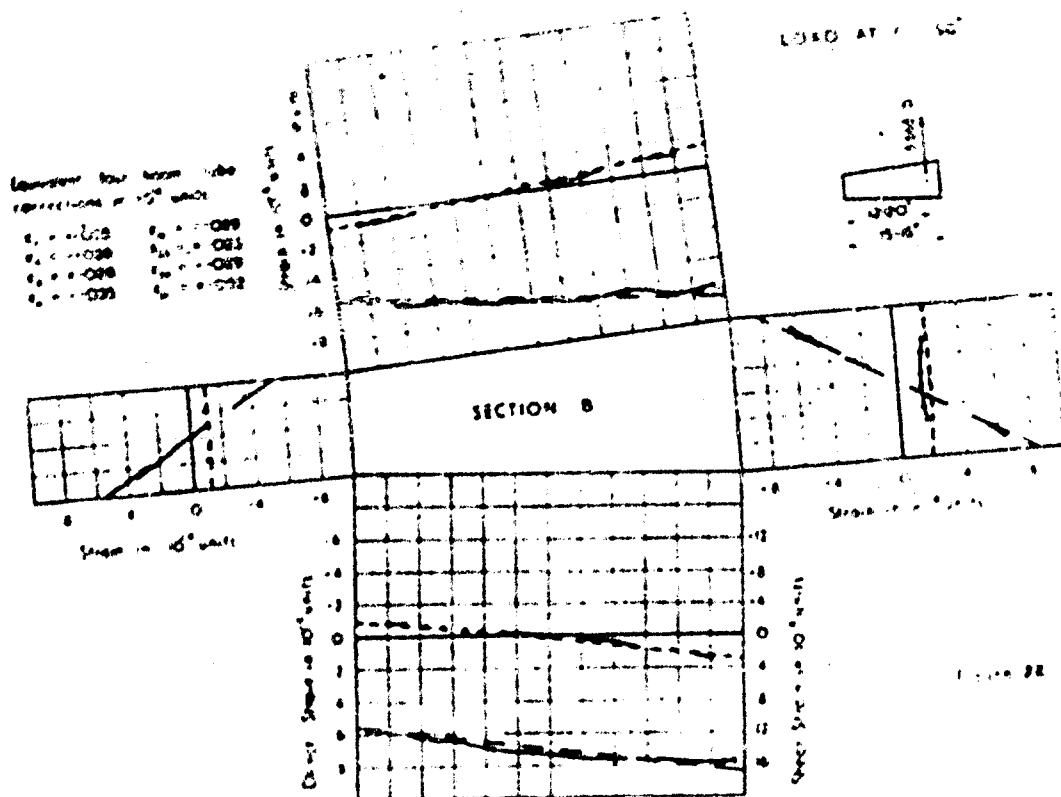


Figure 27



	<u>Direct Strain</u>	<u>Shear Strain</u>	
Experiments	—	—	Tensile strains and compressive shear strains are considered positive and are plotted outwards. The direct strains are drawn full scale and the shear strains half scale.
Theoretical Theory	—	- - -	



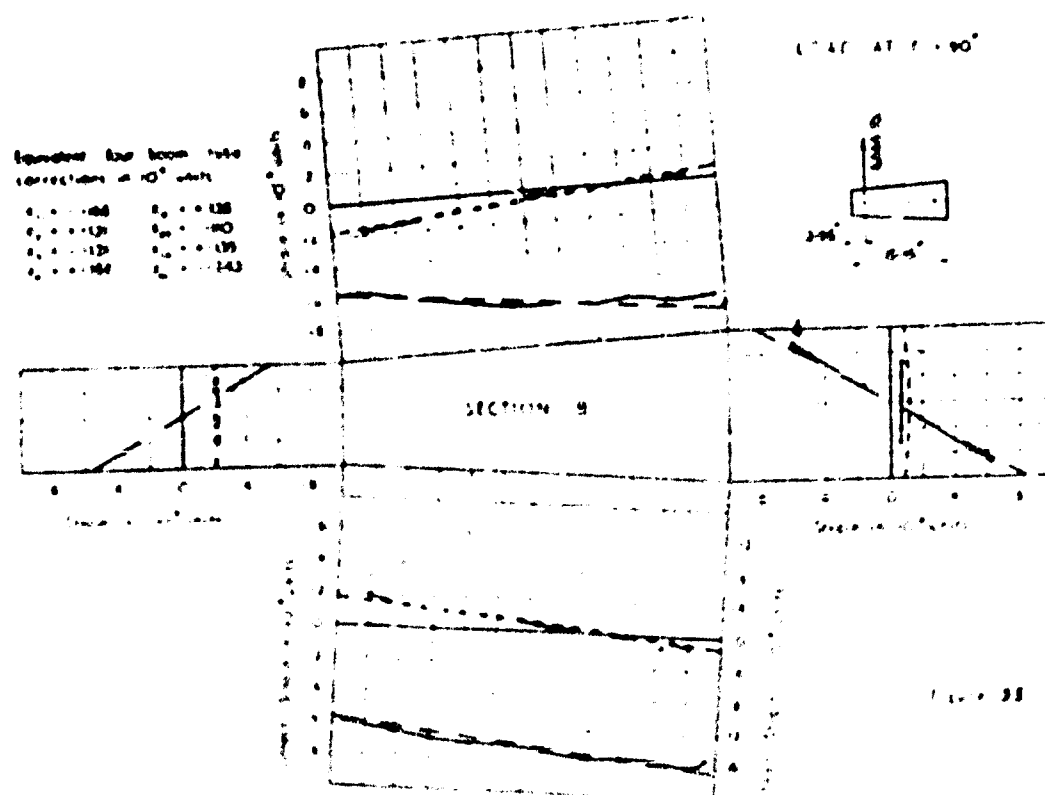


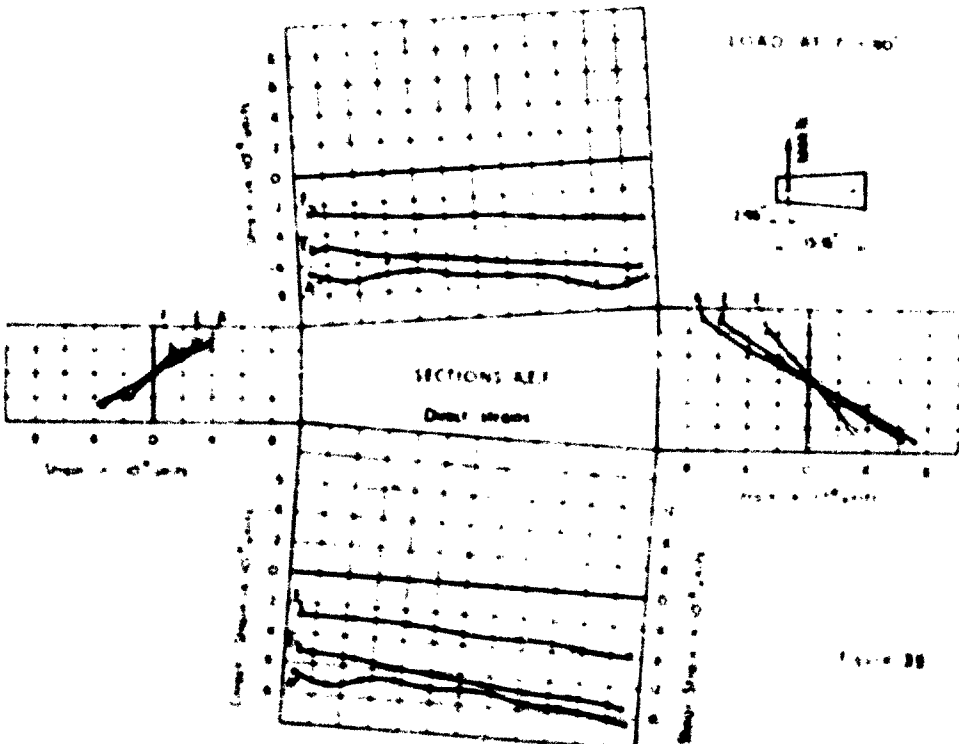
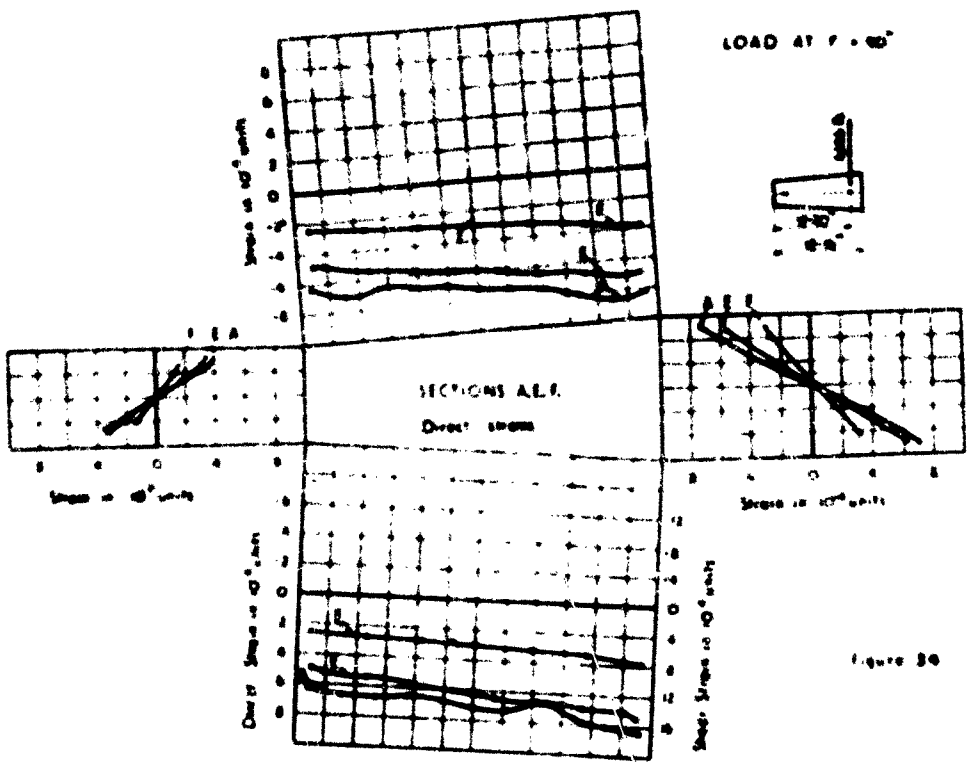
Legend:

—	—	—
—	—	—
—	—	—

Direct Stress      Shear Stress      Tensile stress and compressive stress areas are considered positive and are plotted outwards. The direct stress areas shown in view and the shear stress areas are zero.

Experimental      Elementary Theory





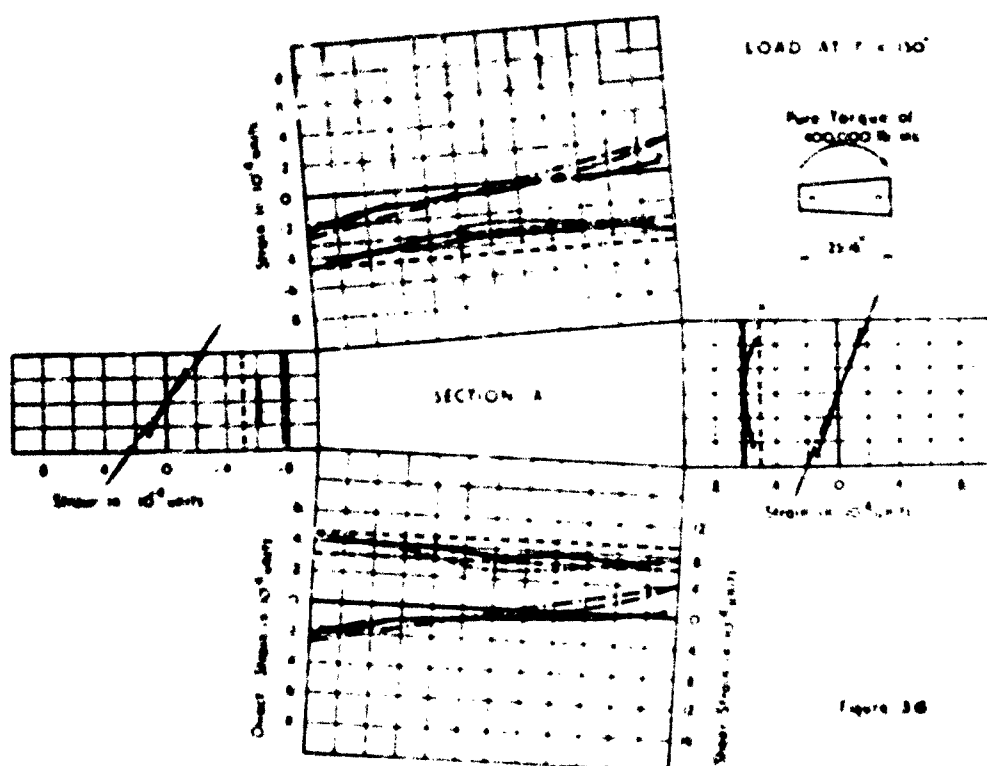
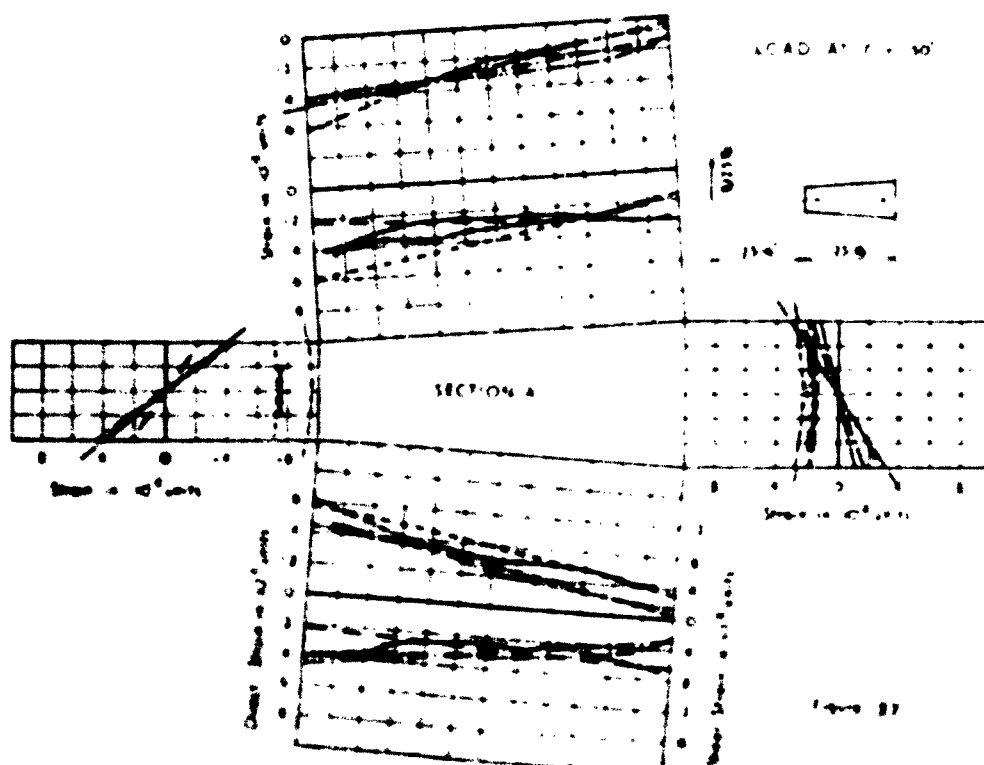


Figure 3.6

	Direct Stress	Shear Stress	
Isoparametric	—	—	Tension stresses and anticlockwise shear stresses are considered positive and are plotted outward.
Elementary Theory	—	—	The direct stresses are drawn full scale and the shear stresses half scale.
Isoparametric Four beam tabs	—	—	
Covers carrying direct stress	—	—	



The curves show readings taken at 15% load and plotted double scale for comparison with the data measured at 50% load.

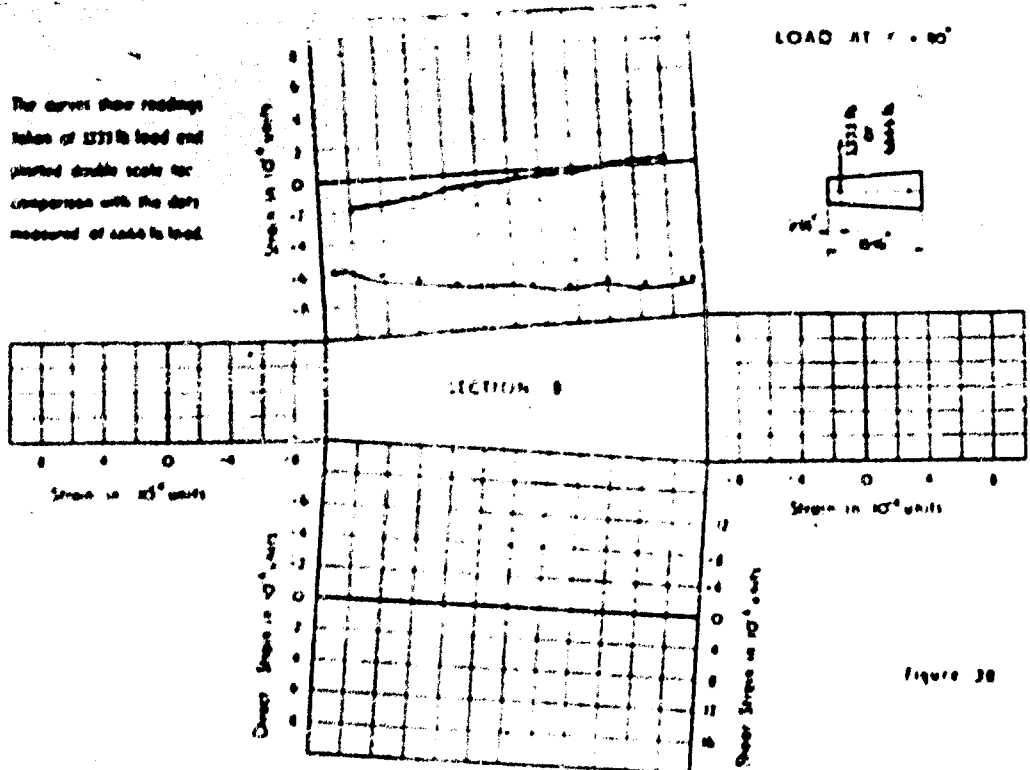


Figure 28

	Direct Strain	Shear Strain
Experiment	—	—
Elementary Theory	- - -	- - -
Equivalent four beam tube	- - -	- - -
Covers slipping direct stress	—	—

Positive strains and anti-clockwise shear strains are considered positive and are plotted outwards. The direct strains are drawn full scale and the shear strains half scale.

Equivalent four beam tube corrections in  $10^{-6}$  units

0.000	0.000
0.000	0.000
0.000	0.000
0.000	0.000

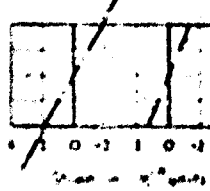
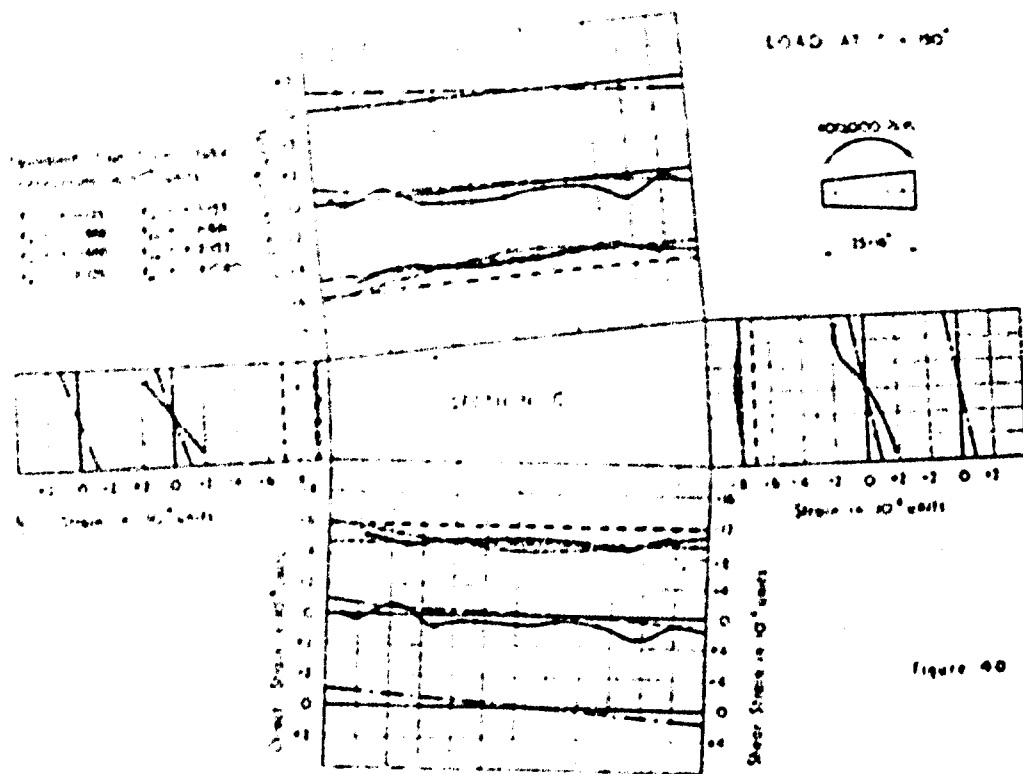
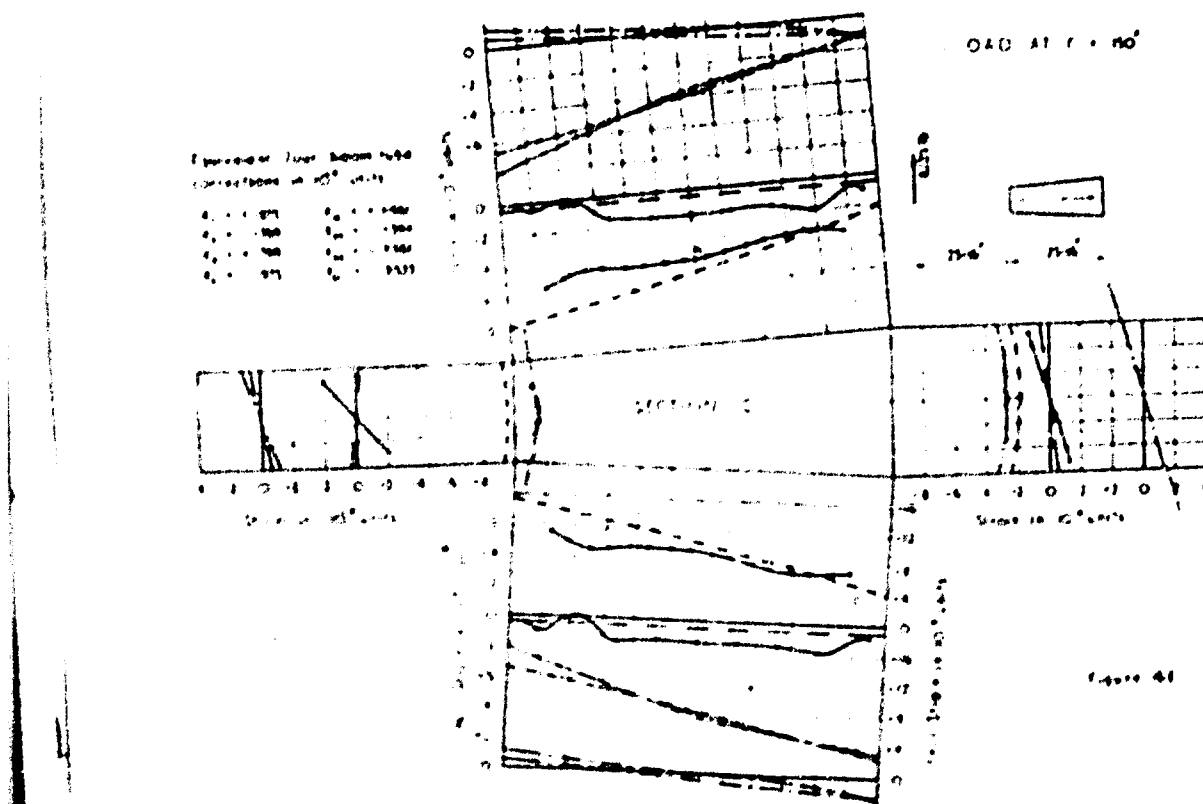
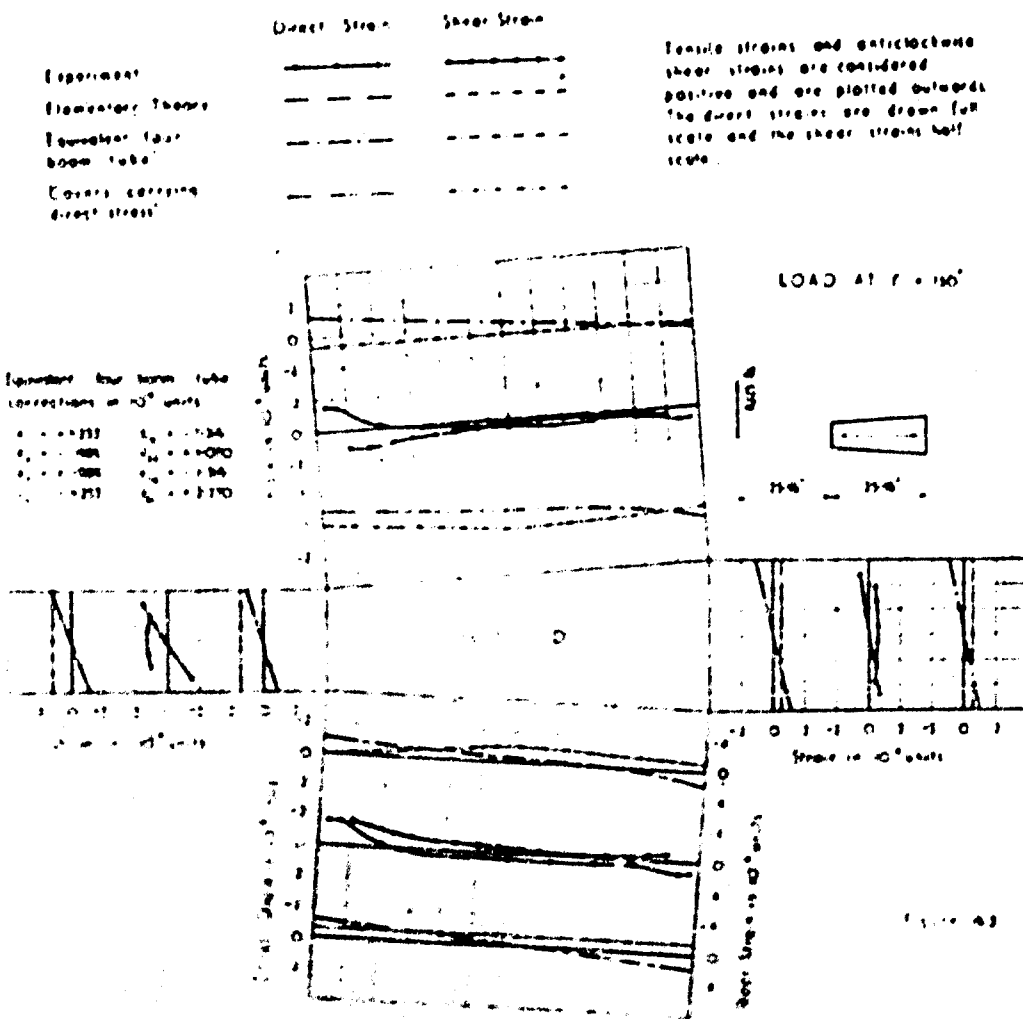
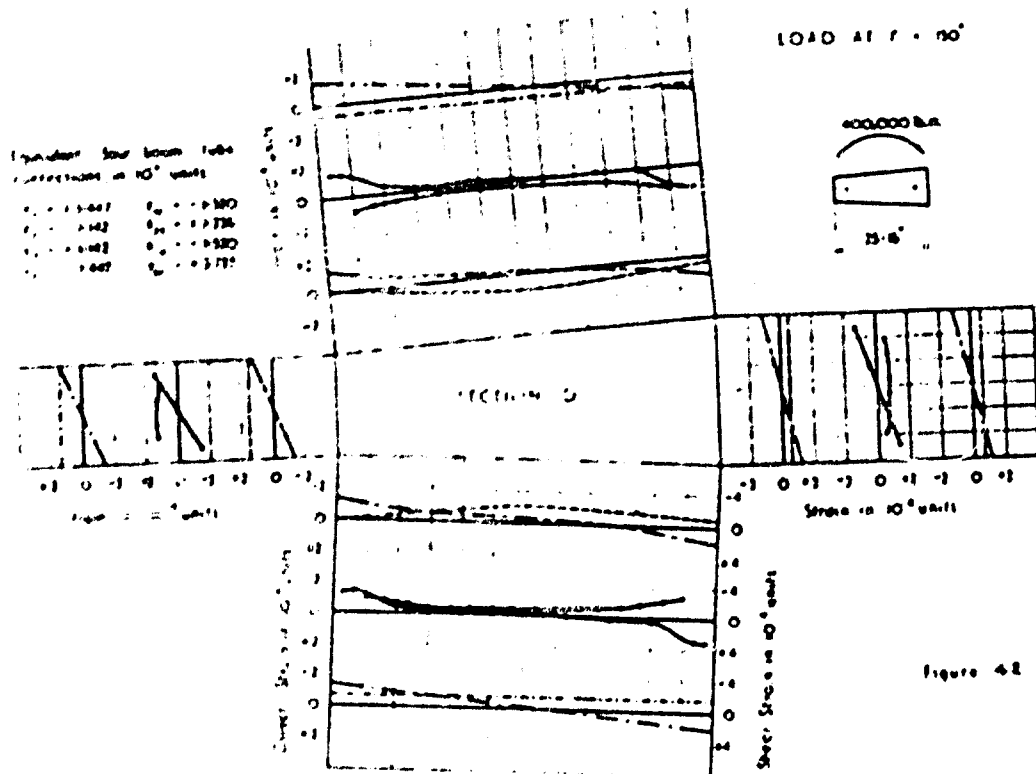


Figure 29



Experiment	Direct Strain	Shear Strain	
Clemente's Theory	—	—	Tensile strains and 'calculated' shear strains are considered positive and are plotted outward.
Isotropic fiber beam tube	—	—	The direct strains are drawn full scale and the shear strains half scale.
Linear isotropic fiber theory	—	—	

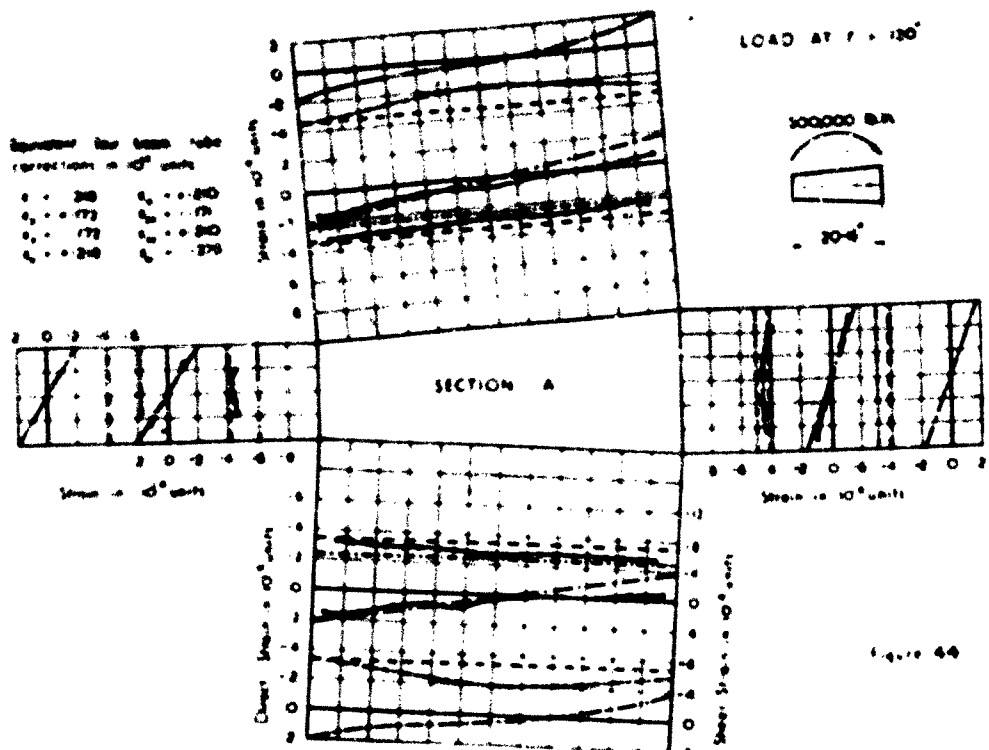




Experiment  
Elementary Theory  
Fourier Four  
beam tube  
Covered covering  
direct stress

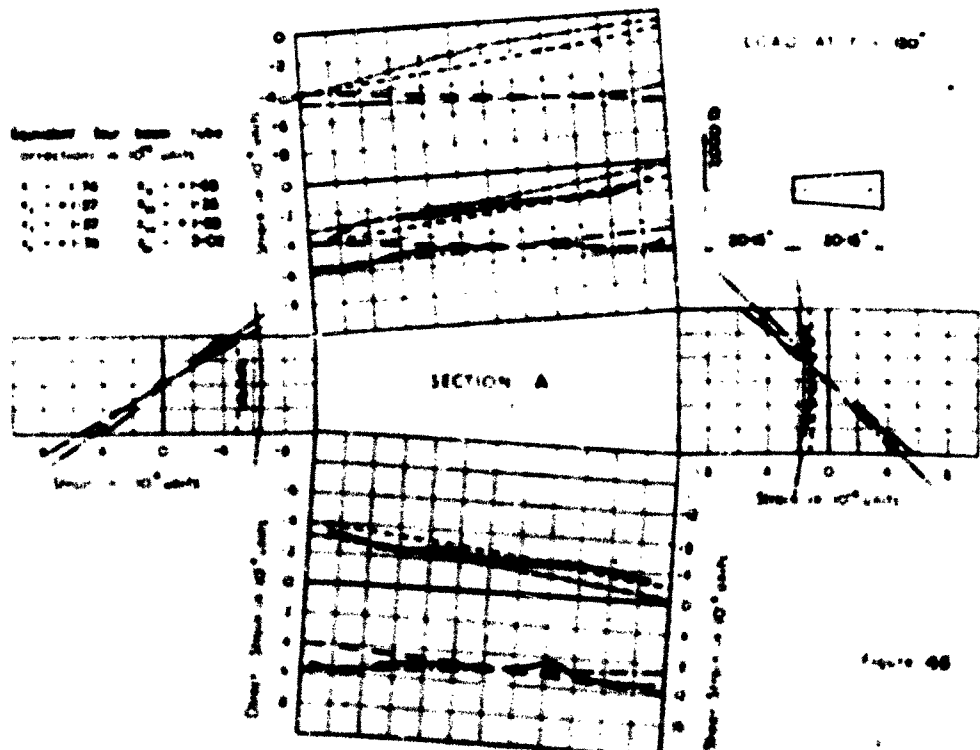
	Direct Stress	Shear Stress
Experiment	—	—
Elementary Theory	—	—
Fourier Four	—	—
beam tube	—	—
Covered covering	—	—
direct stress	—	—

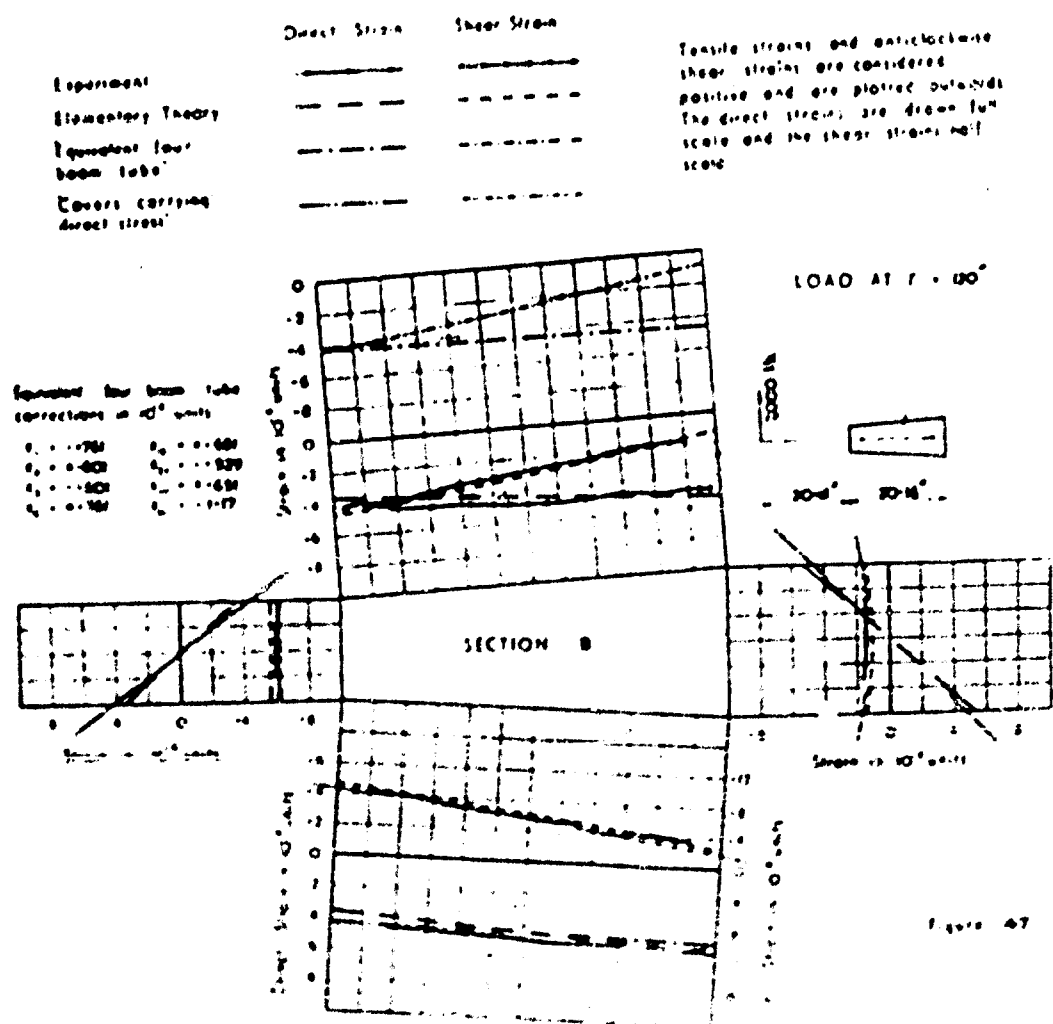
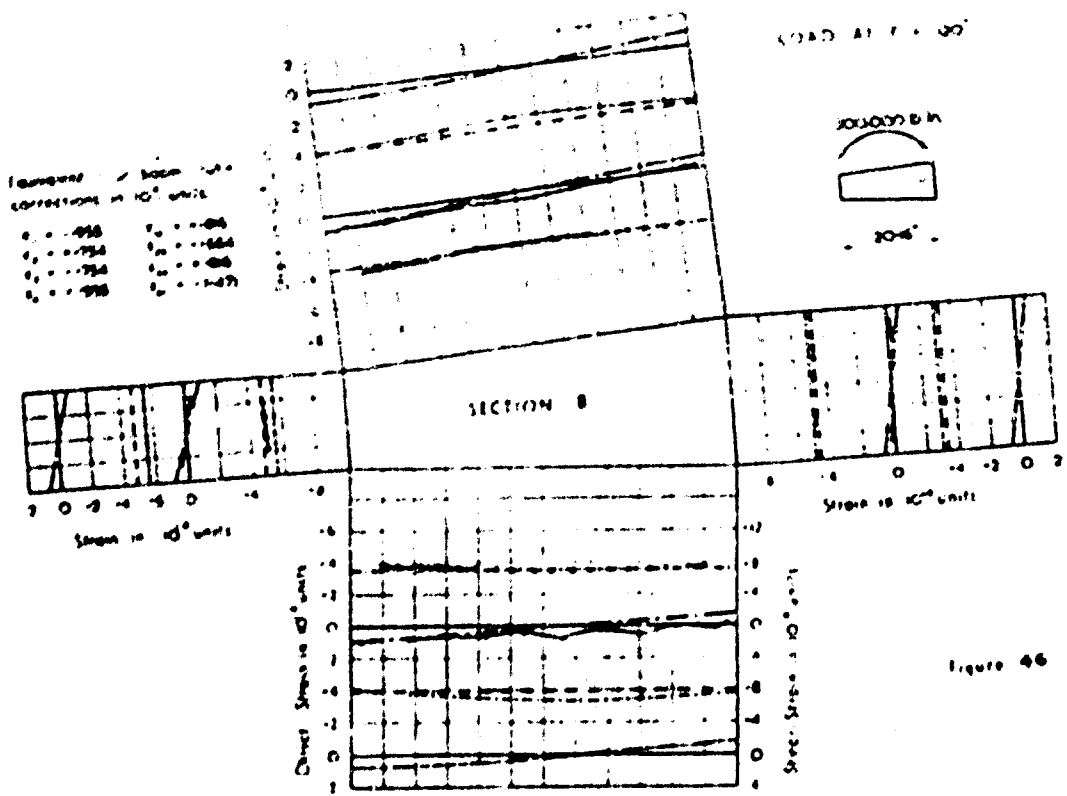
Tensile strains and contractions  
shear strains are considered  
positive and are plotted outward.  
The direct stresses are drawn full  
scale and the shear stresses half  
scale.

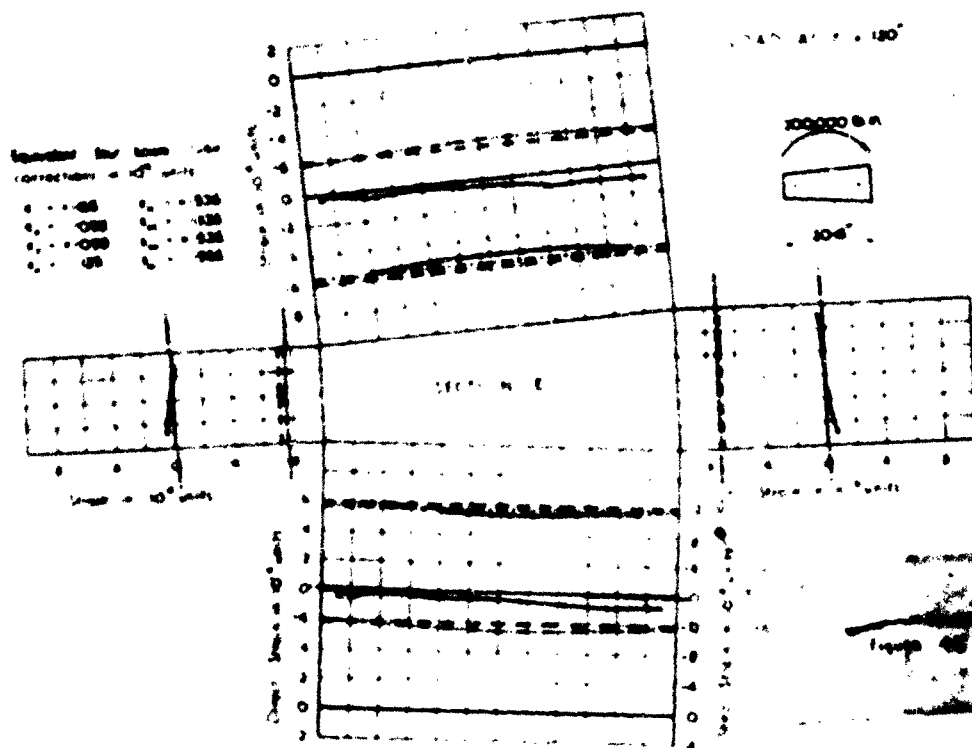


Experiment	Direct Strain	Shear Strain
Elementary Theory	—	—
Concrete Four-beam tube	---	---
Covers carrying direct stress	---	---

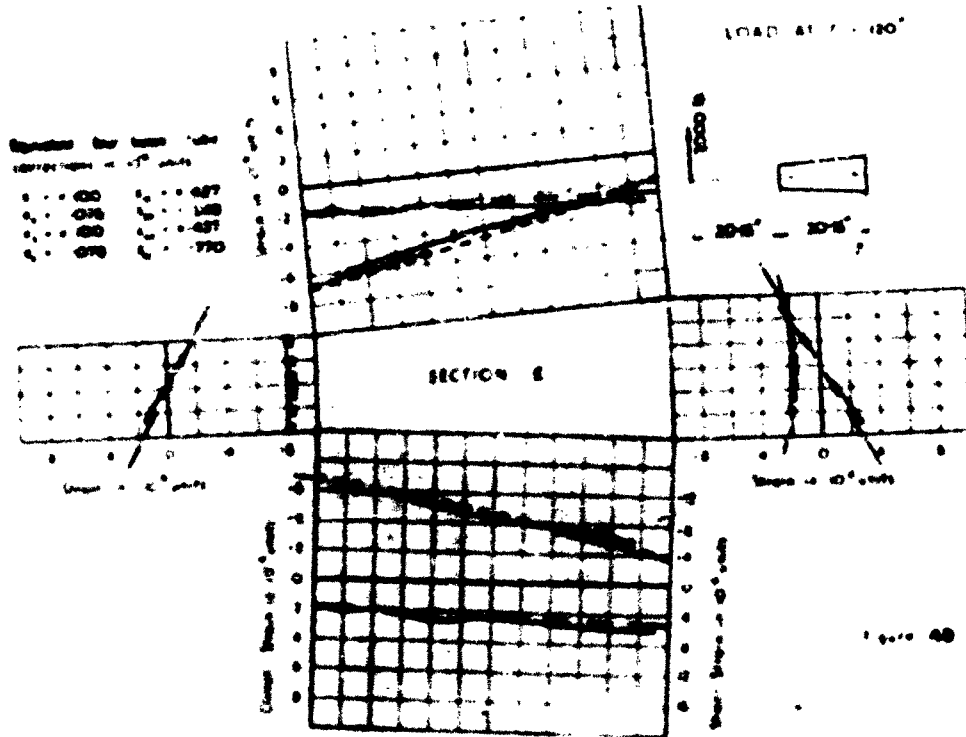
These strain gauges are bonded  
shear strains are measured  
positively and are plotted upward.  
The direct strains are plotted  
downward and the shear strains  
upward.







Tensile strains and compressive shear strains are considered positive and are plotted outwards. The direct strains are drawn full scale and the shear strains half scale.



These curves were  
obtained by superposing  
results for each load  
acting separately.

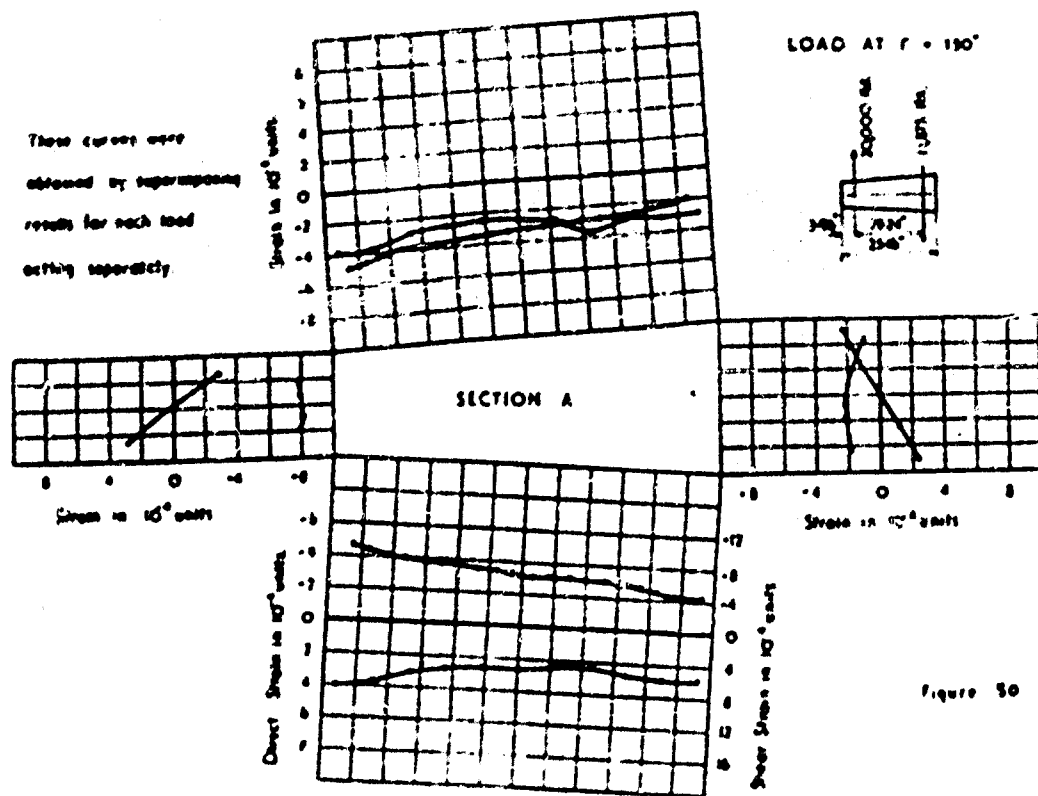


Figure 50

	Direct Strain	Shear Strain
Experiment	—	—
Elementary Theory	- - -	- - -
Taunay's Use beam rule	- - -	- - -
Correct, assuming direct strain	- - -	- - -

Tensile strains and compressive  
shear strains are considered  
positive and are plotted outward.  
The direct strains are drawn to  
scale and the shear strains to  
scale.

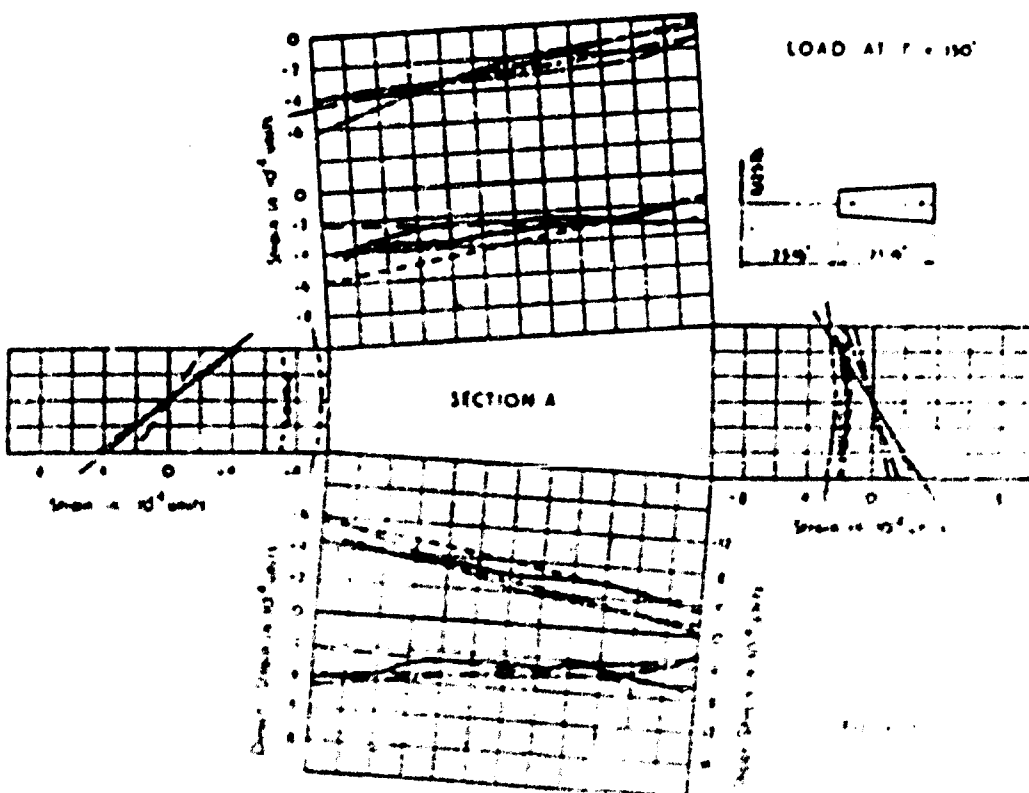


Table 1.

1	2	3	4	5	6	7	8	9	10	11	12	13	14	15	16	17	18	19	20	21	22	23	24	25	26	27	28	29	30	31	32	33	34	35	36	37	38	39	40	41	42	43	44	45	46	47	48	49	50	51	52	53	54	55	56	57	58	59	60	61	62	63	64	65	66	67	68	69	70	71	72	73	74	75	76	77	78	79	80	81	82	83	84	85	86	87	88	89	90	91	92	93	94	95	96	97	98	99	100	101	102	103	104	105	106	107	108	109	110	111	112	113	114	115	116	117	118	119	120	121	122	123	124	125	126	127	128	129	130	131	132	133	134	135	136	137	138	139	140	141	142	143	144	145	146	147	148	149	150	151	152	153	154	155	156	157	158	159	160	161	162	163	164	165	166	167	168	169	170	171	172	173	174	175	176	177	178	179	180	181	182	183	184	185	186	187	188	189	190	191	192	193	194	195	196	197	198	199	200	201	202	203	204	205	206	207	208	209	210	211	212	213	214	215	216	217	218	219	220	221	222	223	224	225	226	227	228	229	230	231	232	233	234	235	236	237	238	239	240	241	242	243	244	245	246	247	248	249	250	251	252	253	254	255	256	257	258	259	260	261	262	263	264	265	266	267	268	269	270	271	272	273	274	275	276	277	278	279	280	281	282	283	284	285	286	287	288	289	290	291	292	293	294	295	296	297	298	299	300	301	302	303	304	305	306	307	308	309	310	311	312	313	314	315	316	317	318	319	320	321	322	323	324	325	326	327	328	329	330	331	332	333	334	335	336	337	338	339	340	341	342	343	344	345	346	347	348	349	350	351	352	353	354	355	356	357	358	359	360	361	362	363	364	365	366	367	368	369	370	371	372	373	374	375	376	377	378	379	380	381	382	383	384	385	386	387	388	389	390	391	392	393	394	395	396	397	398	399	400	401	402	403	404	405	406	407	408	409	410	411	412	413	414	415	416	417	418	419	420	421	422	423	424	425	426	427	428	429	430	431	432	433	434	435	436	437	438	439	440	441	442	443	444	445	446	447	448	449	450	451	452	453	454	455	456	457	458	459	460	461	462	463	464	465	466	467	468	469	470	471	472	473	474	475	476	477	478	479	480	481	482	483	484	485	486	487	488	489	490	491	492	493	494	495	496	497	498	499	500	501	502	503	504	505	506	507	508	509	510	511	512	513	514	515	516	517	518	519	520	521	522	523	524	525	526	527	528	529	530	531	532	533	534	535	536	537	538	539	540	541	542	543	544	545	546	547	548	549	550	551	552	553	554	555	556	557	558	559	560	561	562	563	564	565	566	567	568	569	570	571	572	573	574	575	576	577	578	579	580	581	582	583	584	585	586	587	588	589	590	591	592	593	594	595	596	597	598	599	600	601	602	603	604	605	606	607	608	609	610	611	612	613	614	615	616	617	618	619	620	621	622	623	624	625	626	627	628	629	630	631	632	633	634	635	636	637	638	639	640	641	642	643	644	645	646	647	648	649	650	651	652	653	654	655	656	657	658	659	660	661	662	663	664	665	666	667	668	669	670	671	672	673	674	675	676	677	678	679	680	681	682	683	684	685	686	687	688	689	690	691	692	693	694	695	696	697	698	699	700	701	702	703	704	705	706	707	708	709	710	711	712	713	714	715	716	717	718	719	720	721	722	723	724	725	726	727	728	729	730	731	732	733	734	735	736	737	738	739	740	741	742	743	744	745	746	747	748	749	750	751	752	753	754	755	756	757	758	759	760	761	762	763	764	765	766	767	768	769	770	771	772	773	774	775	776	777	778	779	780	781	782	783	784	785	786	787	788	789	790	791	792	793	794	795	796	797	798	799	800	801	802	803	804	805	806	807	808	809	810	811	812	813	814	815	816	817	818	819	820	821	822	823	824	825	826	827	828	829	830	831	832	833	834	835	836	837	838	839	840	841	842	843	844	845	846	847	848	849	850	851	852	853	854	855	856	857	858	859	860	861	862	863	864	865	866	867	868	869	870	871	872	873	874	875	876	877	878	879	880	881	882	883	884	885	886	887	888	889	890	891	892	893	894	895	896	897	898	899	900	901	902	903	904	905	906	907	908	909	910	911	912	913	914	915	916	917	918	919	920	921	922	923	924	925	926	927	928	929	930	931	932	933	934	935	936	937	938	939	940	941	942	943	944	945	946	947	948	949	950	951	952	953	954	955	956	957	958	959	960	961	962	963	964	965	966	967	968	969	970	971	972	973	974	975	976	977	978	979	980	981	982	983	984	985	986	987	988	989	990	991	992	993	994	995	996	997	998	999	1000

Table 2.

1	2	3	4	5	6	7	8	9	10	11	12	13	14	15	16	17	18	19	20	21	22	23	24	25	26	27	28	29	30	31	32	33	34	35	36	37	38	39	40	41	42	43	44	45	46	47	48	49	50	51	52	53	54	55	56	57	58	59	60	61	62	63	64	65	66	67	68	69	70	71	72	73	74	75	76	77	78	79	80	81	82	83	84	85	86	87	88	89	90	91	92	93	94	95	96	97	98	99	100

Table 3.

1	2	3	4	5	6	7	8	9	10	11	12	13	14	1

## APPENDIX I

### Brief Review of the Argyris and Dusane Theory

For convenience in presentation and use, Argyris and Dusane have given the results of their theory as correction stresses to be superimposed on stresses found by the conventional engineers' theories of bending and torsion. As stress distributions of the conventional theories are statically equivalent to the true stress distributions, the corrections have no statical resultants and have been called 'self balancing' or 'self equilibrating' stresses.

The authors have developed their theory from the conditions for elastic equilibrium of an infinitesimally small element of material. The following simplifying assumptions have been made.

1. If all generators were produced they would meet in a common point outside the tube.
2. The direct stress and strain normal to the generators are zero.
3. The shape of cross section of the tube is maintained by an indefinitely closely spaced system of diaphragms rigid in their own planes but offering no resistance to deflections out of their planes.
4. The diaphragms are all parallel to the root cross section.
5. The angle between any generator and an axis perpendicular to the diaphragms is so small that its square is negligible compared to unity and its cosine may be written as unity.
6. At any point the shear stress along a generator is assumed to have the same value as the shear stress parallel and normal to a diaphragm.
7. The shear modulus is associated with the shear strain parallel to the direction in which the sheet is forced by the diaphragms to be effectively rigid. The direct modulus is associated with the direct strain along generators.

The fundamental assumption of the theory is that the cross sectional shape of a tube is kept constant. From this it follows that the movement under load of any point on the tube can be defined by an axial warping displacement and by the body rotation and displacements of the cross section shape containing the point within its original plane. The three displacements and the rotation appear as variables in the analysis and the strains are written algebraically in terms of their derivatives. As any transverse direct stress in the walls of a tube is assumed to be zero only one equilibrium equation for the stresses at a point has to be satisfied. The major part of the analysis is concerned, in effect, with the solution or approximate solution of this equilibrium equation.

The existence of some stress function,  $\Psi$ , for the tube is assumed which has the form of a function,  $\chi$ , of the distance from the taper point times a function,  $h$ , of the distance around the periphery of the root cross section. By expressing the equilibrium equation in terms of the unknown stress function it has been possible to split it into two separate differential equations, one in terms of the geometry of the root cross section and the other in terms of the distance from the taper point. These give the transverse and longitudinal variations in stress.

178

The equation involving the distance from the taper point has second order derivatives and its solution is not very difficult when the skin thicknesses are either constant or vary in a convenient manner with distance from the taper point.

The equation involving the geometry of the root cross section is linear and differential and has a separate solution with two arbitrary constants for each cell in which the thickness and slope are continuous functions. By considering the compatibility of direct strains and shear flows at each discontinuity around a cross section, an equation can be formed for each of these arbitrary constants. Together with the three equations of statics for equilibrium of the forces in a plane there are  $2n + 3$  linear simultaneous equations for a tube where  $n$  is the number of cells. These equations have non-zero solutions when the determinantal equation is zero. In general the determinantal equation is transcendental and has an infinite number of roots.

The direct stress carrying ability of the walls has been treated analytically for only one specific case - that of a singly symmetrical tube with continuous direct stress carrying covers. In this case formulae are given for the determinantal equation and for the  $h$  function in each wall.

For utility, a localized tube is considered consisting of a number of direct stress carrying rods along generators connected by sheet of a purely shear resistant material. For the idealized tube the equation involving the geometry of the root cross section is algebraic instead of differential and there is only one arbitrary constant for each cell. There are  $n + 1$  simultaneous equations and the determinantal equation has a finite number,  $n + 3$ , of roots. For an idealized tube having more than 6 ~ 8 roots the computation involved would be heavy.

The singular equation for an idealized four box tube has but one root and for this case the theory finds its widest application. Theoretical results for this case have been presented in a form which is immediately convenient for computation.

In general an allowance for the direct stress carrying ability of the walls of a tube may be made by assigning some portion of their cross sectional areas to adjacent boxes or struts. For the case of a four box tube a rational procedure for this has been suggested by Argyris and Durrer.

## APPENDIX II

### Theoretical Computations

The curves of theoretical strain shown superimposed on the graphs of experimental results were computed according to:

- the elementary engineers' theories of bending and torsion,
- the theory of Argyris and Dusane for the case of an equivalent four-boom tube,
- the theory of Argyris and Dusane for the case of a singly symmetrical tube with direct stress carrying top and bottom covers.

A brief record of the results and procedure of computation is given in this Appendix so that the reader may follow the main arguments of the analyses. In the account of the procedure according to Argyris and Dusane he is referred to the appropriate sections and equations of their "General Theory of Cylindrical and Conical Tubes under Torsion and Bending Loads".

#### Elementary theory

The curves for strains by the elementary theories have been obtained from the formulae

$$\frac{\sigma}{E} = \frac{M\bar{y}}{r^2 I_0 E},$$

$$\frac{T_b}{G} = \frac{T_0}{G} - \frac{1}{t_0 I_0 G} \int_0^R t \bar{y} dt,$$

and

$$\frac{r_b}{G} = \frac{r}{2f^2 A_0 t G},$$

where the notation is, see Figs. 3a and 3b.

$r$	distance from taper point
$r_0$	distance from root to taper point
$\rho$	$= r/r_0$
$A_0$	gross sectional area of tube at root
$I_0$	moment of inertia of tube at root
$b$	distance around perimeter of section from an origin at the root cross section

$t$	wall thickness
$\bar{y}$	value of $y$ corresponding to a direct, and shear, elasticity moduli of material
$S$	applied shear force
$K$	bending moment at : section
$M/r$	shear load resisted by direct stress along generators
$Q = (S - M/r)$	shear load resisted by shear stresses
$T$	torsional couple about shear centre
$\sigma$	longitudinal direct stress
$\tau_c$	component of shear stress due to $Q$
$\tau_0$	value of $\tau_c$ at $s = 0$ if $Q$ passed through shear centre
$\tau_b$	component of shear stress due to torque $T$ .

The corner angles, shown in Fig. 3a were considered to be concentrated as loads shown in Fig. 3b. In view of the simplicity of the expressions and as the work was halved by the single symmetry of cross section, shear strains were calculated at as many points around the cross section as seemed desirable (about fifty) for smooth curves to be drawn.

#### Equivalent four-helix tube

An approximation to the axial constraint stresses was made by the method suggested in Appendix A.2.2. of the published theory of Argyris and Dvornic. In discussing it, the notation, figure numbers and equations refer to text of that theory.

The dimensions of cross section which are shown in Fig. 3b of this report were substituted in equations (A20), (A21) and (A22) of the Appendix giving the following box areas corresponding to Fig. 29;

$$B_1 = B_2 = 2.3799, \quad B_3 = 3.3 = 2.0266.$$

These areas and the dimensions of cross section were then substituted in equation (193) of Part A.3 giving

$$\lambda^2 = 0.01693,$$

and with  $\lambda$  in (44)

$$\mu = 0.06135.$$

From (231), (237) and (239) the  $(H)$  functions were found to be

$$\begin{aligned}(H_0)_1 &= +5.163 \quad (H_T)_{12} = +2.115 \\ (H_0)_2 &= -4.074 \quad (H_T)_{23} = -1.720 \\ (H_0)_3 &= +4.074 \quad (H_T)_{34} = +2.115 \\ (H_0)_4 &= -5.163 \quad (H_T)_{41} = -3.810\end{aligned}$$

From (86a),  $v = wr_0 = 16,640$ , the  $G$  functions of (137a) and (137b), obtained with the use of (135a) and (135b) for values of  $r_1 = 90, 120$  and  $150$  at each strain-enriched cross section are

	$\rho_1 = 0.5333$	$\rho_1 = 0.6666$	$\rho_1 = 0.5000$			
$\rho$	$G_\sigma$	$G_T$	$G_\sigma$	$G_T$	$G_\sigma$	$G_T$
0.9833	+0.7763	-0.9164	+0.5652	-0.7950	+0.8696	-0.7939
0.9167	+0.2005	-0.4611	+0.3791	-0.3084	+0.3840	-0.3008
0.7520	-0.3351	-0.6414	+0.1827	-0.1332	+0.2085	-0.1079
0.6139	-0.4306	+0.4306	+0.1107	-0.064	+0.1638	-0.0335
0.7500	-0.1411	-0.1411	-0.0494	-0.026	+0.1412	-0.0120
0.5000	-0.0085	+0.0085	-0.1677	+0.1714	+0.1776	-0.0114
	$G_\sigma^1$	$G_T^1$	$G_\sigma^1$	$G_T^1$		

The correction components of stress were computed from (236a) and (236b) and then superimposed individually on the strains of the elementary theories.

#### Covers carrying direct stress

Correction stresses were also found by the method given in Part 3.8 for a singly symmetrical trapezoidal tube. In this case the direct stress in the covers is considered, but the spar webs are treated as purely shear carrying. To make an allowance for the direct stresses in the webs, the beam areas shown in Fig. 3d, of this report, have been obtained by adding  $1/4$  of each web area to the adjacent beams of Fig. 3c.

By substituting the dimensions shown in the Fig. 3d in equation (46a),  $D = 4,672,600$  and equation (45b) simplified to

$$(-11270.6x^4 + 413.919x^2 + 0.132463) \frac{\sin(\pi x_{12})}{(\pi x_{12})}$$

$$+ (113.266)^2 - 1.42407) \cos(\pi x_{12}) + 1 = 0$$

This equation is transcendental and the first seven roots are

$$\lambda = 0, \quad 0.119328, \quad 0.157646, \quad 0.254259, \quad 0.339556 \\ 0.439595, \quad 0.537617.$$

Solutions for equations (498) to (493) were then computed for each of the six non-zero values of  $\lambda$  and substituted in equations (495), (496) and (496a) in order to find  $H_0$ ,  $H_1$ ,  $(H_r)_{11}$  and  $(H_r)_{41}$ . The  $H$  functions are listed in Table 3 for the webs and for seven equally spaced points across a cover, the dimension  $s$ , shown in the table, is measured from the centre of the cover.

The  $G$  functions were calculated for each of the values of  $\lambda$  from (137a) and (137b) and are listed in Tables 4, 5 and 6 for each strain across a cross section.

Correction stresses were calculated from equations (136a) and (136b), or (319a) and (319b). By taking the first six significant values of  $\lambda$ , the distribution of strain around the cross sections was given by twelve terms of a trigonometric series. Table 7, which has been included as an example, shows the calculation for Section A of the test box when a torque and a shear load were applied separately at  $r = 150$  ( $p_1 = 0.8333$ ). It will be seen from the table that convergence is reasonable for pure torque but is inadequate for bending. Further results for loading at  $r = 150$  are summarised in Table 8.

It had been hoped initially that the terms would have been sufficiently convergent to interpret the shear lag effect in bending. Additional terms could have been computed. However as the labour of computation and tabulation of corrections for the tube with direct stress carrying covers was approximately 800 man hours, it was decided, after an inspection of the theoretical and experimental shear lag effects, that it would be unprofitable to spend further time on this aspect of the problem prior to submitting the report.



Information Centre  
Knowledge Services  
**dstl** Portsmouth,  
Salisbury  
Hampshire  
SP4 0JQ  
02380 62278  
Fax: 02380 623976

Defense Technical Information Center (DTIC)  
8725 John J. Kingman Road, Suit 0944  
Fort Belvoir, VA 22060-6218  
U.S.A.

AD#: AD011549

Date of Search: 30 May 2008

Record Summary: DSIR 23/20965

Title: Transversely Stiffened Tapered Box Girder under Torsion and Bending

Availability Open Document, Open Description, Normal Closure before FOI Act: 30 years

Former reference (Department) ARC 15128

Held by The National Archives, Kew

This document is now available at the National Archives, Kew, Surrey, United Kingdom.

DTIC has checked the National Archives Catalogue website (<http://www.nationalarchives.gov.uk>) and found the document is available and releasable to the public.

Access to UK public records is governed by statute, namely the Public Records Act, 1958, and the Public Records Act, 1967.

The document has been released under the 30 year rule.

(The vast majority of records selected for permanent preservation are made available to the public when they are 30 years old. This is commonly referred to as the 30 year rule and was established by the Public Records Act of 1967).

**This document may be treated as UNLIMITED.**